

# A Statistical Model of Bipartite Networks: Application to Cosponsorship in the United States Senate\*

Adeline Lo<sup>†</sup> Santiago Olivella<sup>‡</sup> Kosuke Imai<sup>§</sup>

## Abstract

Many networks in political and social research are bipartite, with edges connecting exclusively across two distinct types of nodes. A common example includes cosponsorship networks, in which legislators are connected indirectly through the bills they support. Yet most existing network models are designed for unipartite networks, where edges can arise between any pair of nodes. However, using a unipartite network model to analyze bipartite networks, as often done in practice, can result in aggregation bias and artificially high-clustering — a particularly insidious problem when studying the role groups play in network formation. To address these methodological problems, we develop a statistical model of bipartite networks theorized to be generated through group interactions by extending the popular mixed-membership stochastic blockmodel. Our model allows researchers to identify the groups of nodes, within each node type in the bipartite structure, that share common patterns of edge formation. The model also incorporates both node and dyad-level covariates as the predictors of group membership and of observed dyadic relations. We develop an efficient computational algorithm for fitting the model, and apply it to cosponsorship data from the United States Senate. We show that legislators in a Senate that was perfectly split along party lines were able to remain productive and pass major legislation by forming non-partisan, power-brokering coalitions that found common ground through their collaboration on low-stakes bills. We also find evidence for norms of reciprocity, and uncover the substantial role played by policy expertise in the formation of cosponsorships between senators and legislation. We make an open-source software package available that makes it possible for other researchers to uncover similar insights from bipartite networks.

**Keywords:** bipartite network, mixed-membership model, social network, stochastic blockmodel, variational inference, Congress, cosponsorship

---

\*The methods described in this paper can be implemented via the open-source statistical software, NetMix, available at <https://CRAN.R-project.org/package=NetMix>. The authors are grateful for comments from Alison Craig, Skyler Cranmer, Sarah Shugars and the participants of the Harvard IQSS Applied Statistics seminar.

<sup>†</sup>Assistant Professor of Political Science, UW-Madison. Email: [aylo@wisc.edu](mailto:aylo@wisc.edu), URL:<https://www.loadline.com/>

<sup>‡</sup>Associate Professor of Political Science, UNC-Chapel Hill. Email: [olivella@unc.edu](mailto:olivella@unc.edu)

<sup>§</sup>Professor, Department of Government and Department of Statistics, Harvard University. 1737 Cambridge Street, Institute for Quantitative Social Science, Cambridge 02138. Email: [imai@harvard.edu](mailto:imai@harvard.edu), URL:<https://imai.fas.harvard.edu/>

# 1 Introduction

Bipartite networks — or networks in which ties connect actors of two distinct types, and no such connections occur between actors of the same type — are commonly encountered in political and social research. Examples include individuals who belong to different ethnic groups (e.g. Larson, 2017), policies adopted by U.S. states (e.g. Desmarais, Harden, and Boehmke, 2015), and product-level trade between countries (e.g. Kim, Liao, and Imai, 2020). Such networks, sometimes known as affiliation networks, are also common in other domains: customer-product relationships (e.g Huang, Li, and Chen, 2005), actor-movie ties (e.g. Peixoto, 2014), and even document-word occurrences of the kind typically used in text-as-data analyses (e.g. Lancichinetti et al., 2015) can be represented as bipartite networks.

Despite their ubiquity, the most popular approach to analyzing a bipartite network is to aggregate them to a *unipartite* network, containing information about the relationships among only one type of node. Consider a stylized example of bipartite network depicted in panel (b) of Figure 1, in which legislators (circles) and bills (triangles) represent two separate types of nodes with cosponsorship ties occurring only between the two types rather than within each type. Researchers often *project* these bipartite network data onto a unipartite network of legislators. Panel (a) of Figure 1 shows the resulting projected unipartite network, in which an edge between two legislator nodes captures the total number of cosponsored bills between them (see, e.g., Tam Cho and Fowler, 2010; Muraoka, 2020).

Such projections are a common practice whenever researchers analyze naturally bipartite networks. After examining recent publications in top political science journals, we find that 26 (or 28%) of the 93 articles that model relational data as an outcome examine bipartite networks, in which there are two mutually-exclusive actor types and connections occur only across (rather than within) types. Among these studies, all but one perform a projection onto a unipartite network (see Table A.1 in Appendix A.1, which includes information on each of the two actor types in the corresponding bipartite examples, such as trade networks that connect individual *countries* to specific *products*).

The popularity of this projection strategy is not surprising, given that the most commonly used statistical

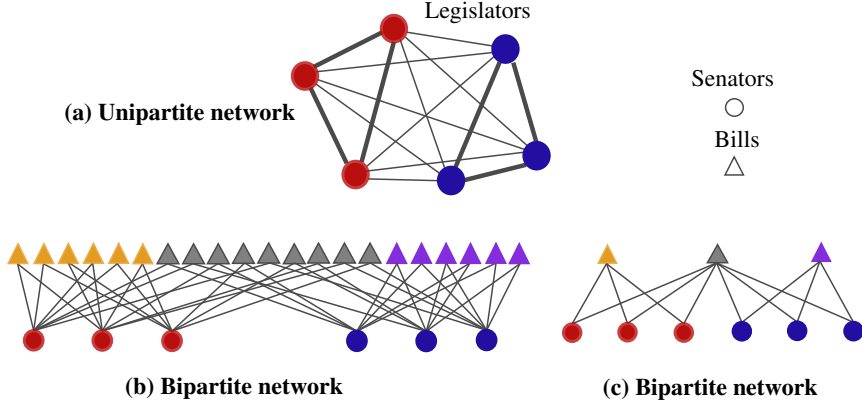


**Figure 1: Illustrative example networks representing cosponsorship of bills in bipartite and unipartite forms.** Two very different bipartite networks in panels (b) and (c) result in the same unipartite network shown in panel (a) when projected. The unipartite network loses the information about the types of bills cosponsored by the senators (indicated by the color of each triangle) and the information about cosponsorships themselves (e.g., the number of cosponsors, number of cosponsored bills).

models of static network formation in the social sciences — typically some variant of the latent-space model (Hoff, Raftery, and Handcock, 2002) or the exponential random graph model (or ERGM; Frank and Strauss, 1986; Wasserman and Pattison, 1996) — were originally designed for unipartite networks. This is also true for more recently proposed modeling approaches to network cross-sections, including the generalized ERGM (Desmarais and Cranmer, 2012), the additive and multiplicative effects model (Minhas, Hoff, and Ward, 2019), the stochastic blockmodel (SBM) (e.g., Karrer and Newman, 2011), and the dynamic mixed membership stochastic blockmodel (dynMMSBM) (Olivella, Pratt, and Imai, 2022).

Unfortunately, the projection of a bipartite network onto a unipartite network leads to substantial loss of information, possibly resulting in misleading estimates of the determinants of network ties (e.g. Marrs et al., 2020). This can be illustrated by the fact that in Figure 1, two completely different bipartite networks shown in panels (b) and (c) result in the same unipartite network presented in panel (a). Moreover, such projections are known to result in networks with spuriously high clustering coefficients (e.g. Newman, Strogatz, and Watts, 2001; Guillaume and Latapy, 2004) — producing incorrect estimates of network community structure and polarization. This is particularly important when theories about the determinants of network formation focus on the role played by groups, communities, or coalitions, and the extent to which they may exhibit fragmentation or cohesion (e.g., González-Bailón and Wang, 2016; Larson et al., 2019;

Sunstein, 2009; Sunstein, 2018).

To minimize the risks brought about by these issues and avoid the need for projections altogether, we extend the popular mixed membership stochastic blockmodel (MMSBM; Airoldi et al. 2008, and *dynMMSBM*; Olivella, Pratt, and Imai 2022) to bipartite networks, in which groups are theorized to play an influential role. The proposed model, which we call *biMMSBM*, allows researchers to discover the groups of nodes, within each node type or family, that share common probabilistic patterns of edge formation (so called *stochastic equivalence classes*). In the aforementioned cosponsorship example, the model characterizes how different communities of legislators cosponsor different types of bills — thus classifying legislators and bills into their own, substantively meaningful groups — without artificially resulting in evidence of a polarized and hyper-partisan congress.<sup>1</sup>

The *biMMSBM* is based on a mixed-membership (or admixture) structure, where a node of one type can belong to different latent groups depending on which nodes of the other type they are interacting with. This flexibility allows us to capture nuanced social interactions, in which actors adopt different roles when interacting with others. It also sets our model apart from most of the existing bipartite community detection models that assume every node (or every edge) belongs to a single group (e.g. Govaert and Nadif, 2003; Larremore, Clauset, and Jacobs, 2014; Zhou and Amini, 2019; Kim and Kunisky, 2020).<sup>2</sup> In cosponsoring networks, for example, a legislator may cooperate with a different group of colleagues when considering the cosponsorship of bills in different policy areas. Our model can capture the complexity of social networks through a wide range of edge formation patterns, and is particularly well-suited for connectivity patterns that result from the existence of latent classes, or communities (such as legislative coalitions).

---

<sup>1</sup>As such, our model complements recently developed modeling strategies for bipartite graphs that nevertheless have different inferential goals. A good example is the literature that tries to identify the most important subgraph, or “backbone”, of bipartite networks (see, for instance, Neal, 2014a)

<sup>2</sup>Allowing for mixed-memberships (a kind of constrained latent space) also sidesteps the serious estimation issues common in ERGM-style modeling approaches (Schweinberger, 2011; Chatterjee and Diaconis, 2013). Issues like inferential degeneracy and ill-behaved likelihood surfaces, which plague unipartite ERGMs, are also present in their bipartite extensions — even after resorting to common regularization strategies (such as geometric weighting; see, for instance, Skvoretz and Faust, 1999; Wang et al., 2009).

In addition, our model allows the use of covariates to explain the patterns of edge formation between nodes of different types (White and Murphy, 2016; Razaee, Amini, and Li, 2019). More specifically, our model incorporates two types of covariates. First, one can use node-level covariates to characterize learned group memberships. In the cosponsorship example, we can use the characteristics of legislators (e.g., their ideology and partisanship) and those of bills (e.g., their policy contents or author characteristics) to understand the determinants of their respective membership into discovered communities. Second, the model also allows incorporating dyadic covariates to directly predict edge formation and relax the assumption that latent group structures are solely responsible for generating the network. This feature is helpful when a theoretically relevant variable is defined for a pair of nodes of different types (e.g., whether a legislator is a member of the committee(s) a bill was originally referred to).

In contrast, many existing modeling approaches force researchers to adopt a two-step analytic strategy, conducting standard regression analyses of network model outputs (e.g. Maoz et al., 2006; Handcock, Raftery, and Tantrum, 2007; Zhang et al., 2008; Cao, 2009; Tam Cho and Fowler, 2010; Battaglini, Scialabazza, and Patacchini, 2020). The few approaches that could accommodate bipartite networks and both nodal and dyadic covariates either lack available software implementations (e.g., the otherwise excellent AME model of Hoff, 2021) or suffer from issues inherited from their unipartite counterparts (e.g., the bipartite ERGM model first proposed by Agneessens, Roose, and Waege, 2004, implemented in the R package `ergm`, can experience severe practical issues of degeneracy and misspecification). By offering a single-step, comprehensive approach to network data analysis that explores a well-behaved posterior distribution, our model can be readily used by applied researchers who wish to test theories about the role of groups in the process of network formation, or make predictions on new sets of actors.

One disadvantage of MMSBM-type network models is that a fully Bayesian inference strategy relying on Markov chain Monte Carlo simulation is computationally prohibitive for networks of medium or large size. To overcome this, we follow the computational strategy used in the existing methodological literature and develop a computationally efficient variational Bayes approximation to our model's collapsed posterior using stochastic optimization (Teh, Newman, and Welling, 2007; Airoldi et al., 2008; Hoffman et al., 2013;

Gopalan and Blei, 2013; Olivella, Pratt, and Imai, 2022). We implement this fitting algorithm in the open-source software package `NetMix` (Olivella, Lo, et al., 2021) so that researchers can use the proposed model in their own research.

To illustrate the potential of `biMMSBM` to study political interrelations, we fit the model to a network generated by cosponsorship decisions in the U.S. Congress. As coalitions are at the heart of legislative politics (Riker, 1962), a model that is designed to identify and explain latent groups is best suited to capture the politics of legislative support that underlie these cosponsorship decisions. More specifically, we study the patterns of legislative cosponsorship during the penultimate instance of a perfectly split Senate in U.S. history — the 107th Congress. We model the bipartite network connecting Senators to legislation (or “bills”) through the discovery of latent groups, while examining the roles of Senator characteristics (party, ideology, seniority, and gender, bill characteristics (time of introduction, the party, ideology, seniority, and gender of the bill’s sponsor; and the bill’s substantive topic), and Senator-bill dyadic features (reciprocity and shared legislative committees).

Contrary to the results of a unipartite network analysis, our modeling strategy identifies a group of senators who collaborate across party lines to cosponsor low-stakes legislation (including symbolic resolutions), which in time opens a path for more contentious legislation to be considered. Specifically, we identify the important role played by up-and-rising junior senators from both parties in generating cross-aisle collaboration. Beyond the substantial role played by this group of junior power brokers and the set of low-stakes legislation they use to build a common ground, we also identify the critical role of shared committee memberships, and find evidence of bill-specific norms of reciprocity in cosponsorship — a phenomenon that would be lost if one focuses on the projected univariate network measures.

In what follows, we discuss this motivating application — the politics of cosponsorship in the U.S. — and explain the risk of aggregation bias and artificial inflation of network clustering when projecting bipartite networks to unipartite ones (Section 2). We then present the details of our modeling approach in Section 3, and the results of our empirical analysis of the cosponsorship network during the 107th Congress in Section 4. Finally, in Section 5, we conclude with a discussion about the applicability of our model to

other domains and future research.

## 2 The Cosponsorship Network Among Senators

In this section, we introduce the cosponsorship network data among legislators in the U.S. Senate, which serves as our motivating example. We point out the bipartite nature of the data and explain why projecting this bipartite network onto a unipartite one results in loss of information, an incorrect (and inflated) notion of how polarized relations are, and possibly aggregation bias.

### 2.1 Background

Cosponsorship relationships among U.S. senators offer a useful window into their legislative interests and goals, as they indicate willingness to publicly and directly endorse a particular piece of legislation (see e.g., Koger, 2003; Tam Cho and Fowler, 2010; Arnold, Deen, and Patterson, 2000; Kirkland, 2011). For senators, cosponsorship is important because the rules of the Senate constrain sponsorship to a single legislator. Thus, cosponsorships often indicate broader support for the content of the legislation or sponsoring legislator, increases media attention, and generates a credible commitment device (Krutz, 2005; Bernhard and Sulkin, 2013a). In the Senate, the 60-vote threshold super-majority required to overcome the threat of a filibuster further enhances the importance of cosponsorships — especially bipartisan ones (Rippere, 2016a).

Furthermore, previous work has noted the importance of collaboration among senators in legislative productivity and influence (Fowler, 2006; Holman, Mahoney, and Hurler, 2022) and the costs of renegeing on cosponsorships (Bernhard and Sulkin, 2013b). Although there are limits to what cosponsorships can help us understand (for instance, Wilson and Young (1997) and Anderson, Box-Steffensmeier, and Sinclair-Chapman (2003) suggest limits to how much cosponsorship can predict ultimate bill passage), there is enough evidence to suggest that cosponsorship decisions meaningfully affect legislators' overall effectiveness as lawmakers (e.g., Harbridge-Yong, Volden, and Wiseman, 2023), and have been touted as one of the clearest forms of non-strategic issue positioning among legislators (Desposato, Kearney, and Crisp, 2011; Lawless, Theriault, and Guthrie, 2018).

Accordingly, scholars have been interested in establishing the determinants of cosponsorship (see,

among others, Campbell, 1982; Krutz, 2005; Grossmann and Pyle, 2013; Fong, 2020). Here, we study cosponsorship to understand partisan gridlock and collaborative behaviors in the Senate. In particular, we are interested in the extent to which patterns of cosponsorship exhibit cross-party cooperation when the Senate faces potential stalemate on account of partisan divisions. What do these cosponsorship networks tell us about the ways in which hyper-partisanship can be overcome? Can a senate remain productive even in the face of a perfect partisan split? Any viable answer to these questions must consider the full extent of collaboration, including potential heterogeneity over the kinds of legislation senators choose to collaborate on.

This last point is important, because such heterogeneity is common in cosponsorship networks. Consider, for example, the two sample bipartite networks in Figure 2. These are drawn from the full network of cosponsorships during 107th Congress, which was in session between 2001 and 2003, as the presidency transitioned from the Clinton to the Bush administration.<sup>3</sup> The networks in both panels contain all 100 senators (left-side nodes) and two samples of bills (right-side nodes). On the left panel, we look at senator-bill bipartite patterns for bills that are heavily partisan in cosponsorship — either primarily cosponsored by Republicans or by Democrats only). On the right, Figure 2 presents bipartite patterns for bills that are heavily *bipartisan* in cosponsorship. Over these two subsets of bills, we observe substantial heterogeneity in cosponsorship behaviors: while a few bills attract many cosponsors (represented by multiple drawn edges to the bill), many more have relatively few.<sup>4</sup> Some bills are highly bipartisan, while others find support mainly

---

<sup>3</sup>The 107th Senate was eventful by many standards. Aside from battles over health care policy, education bills and investigations and rewriting of election laws after the tumultuous 2000 presidential election, party control of the Senate changed hands as well. During the two years, control of the Senate flipped from a narrow Republican control where the G.O.P. could mostly enact policy through convincing a handful of Democrat colleagues in a 50-50 Senate split (where Vice President Dick Cheney gave the Republicans their narrow edge) to a likewise razor-thin advantage towards the Democrats in June 2001 once Jim Jeffords (R/I-VT) defected from the Republican party as an Independent and began to caucus in earnest with Democrats. Finally, 9/11 shook the domestic agenda altogether, and ramped up foreign policy and security as priority in both parties, seeing the beginnings of the subsequent “War on Terror.” Given the important shifts in power and legislative activity that occurred during this Senate, it serves as a hard case to evaluate our model.

<sup>4</sup>More formally, the degree distribution of bills is best captured using a power law, with many bills having few cosponsors no bills, and a few bills being cosponsored by many senators. In contrast, the degree distribution of senators is far less heavy tailed,

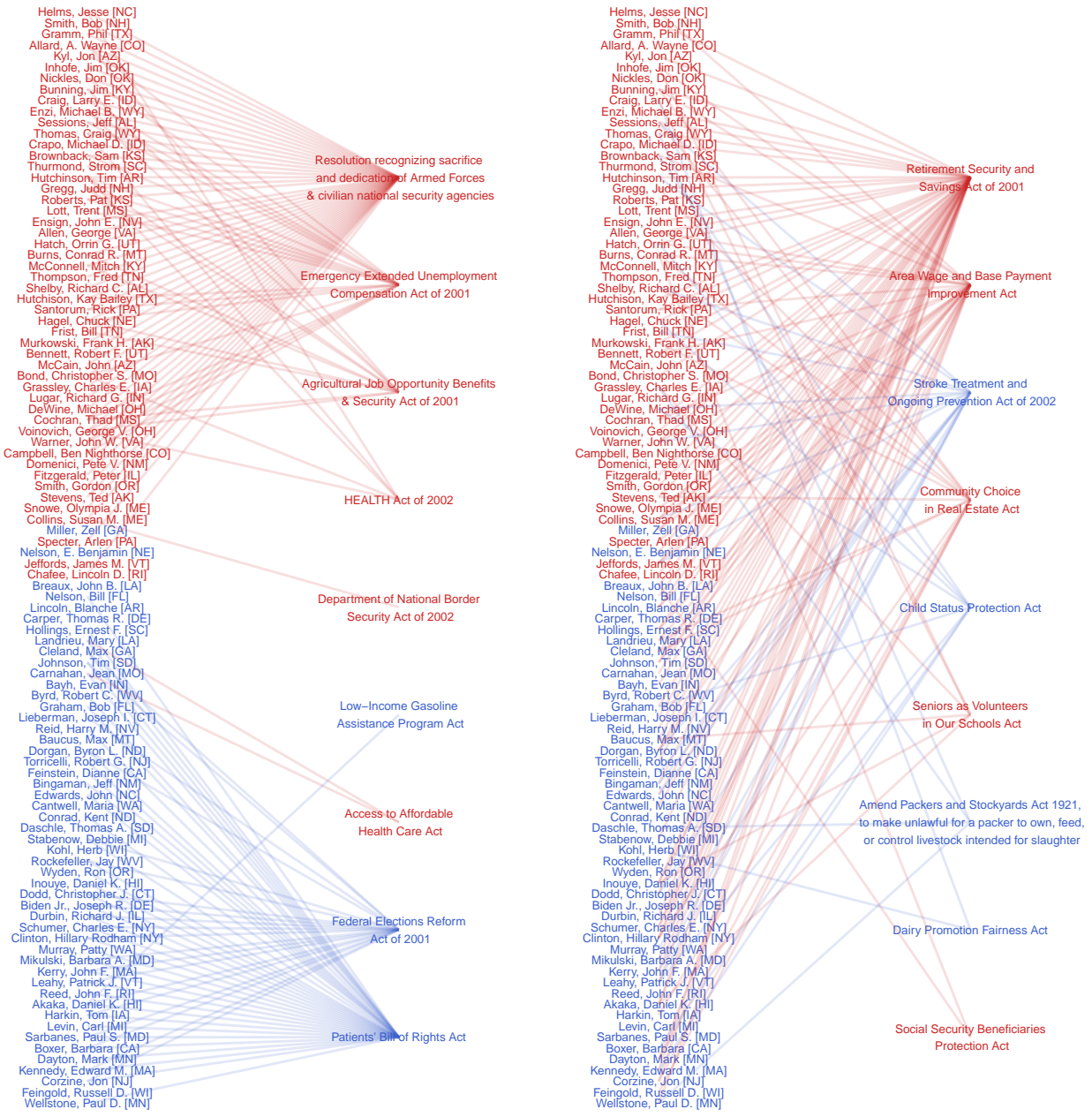


**Figure 2: Cosponsorship Networks among Senators in the 107th Congress.** The figure depicts two bipartite networks sampled from the 107th Congress, with all 100 senators sorted by ideology (most conservative senators at the top), and a sample of bills sorted based on node degree. The left panel presents a sampled network in which bills are heavily partisan in their cosponsorship compositions — either primarily cosponsored by Republicans or by Democrats — while the right panel presents a sample of bills that are highly bipartisan in their cosponsorship compositions. These networks illustrate the large heterogeneity in both composition and degree across bill nodes in our network.

within a single party.

As shown next, if we were to aggregate over bills — by projecting the bipartite cosponsorships onto a network among senators as commonly done — all of this heterogeneity would be lost. If cross-party collaboration is systematically associated with whatever brings about this heterogeneity, we risk painting an incorrect picture of how partisanship drives collaboration among legislators.

## 2.2 Projection onto a unipartite network can be misleading

Despite this risk, the most common approach to studying bipartite networks is to project them onto unipartite ones. In the current application, one may turn the senator-bill bipartite network into senator-only unipartite graph where an edge between two senators represents whether or not they cosponsor a bill together (or the number of bills, for a weighted projection; see e.g., Tam Cho and Fowler, 2010). In adopting this strategy, however, researchers risk losing relevant bill-specific and senator-bill pair-specific information that may be useful in understanding decisions to cosponsor, including the policy content of individual bills, the timing in which bills are introduced and endorsed by legislators, and the extent to which collaboration happens through widely popular pieces of legislation (Neal, 2014b; Neal, 2020; Kirkland and Gross, 2014).

Thus, aggregating over potentially relevant heterogeneity in bill- and senator-bill level data can lead to incorrect substantive takeaways. To see how this may be the case, revisit the stylized scenario presented in Figure 1 of Section 1. A simple weighted unipartite representation of a cosponsorship network appears in panel (a) of the figure. In this graph, the circle nodes representing senators have weighted edges connecting them to cosponsored triangle bills, with weights given by the number of such cosponsorships. The colors of senator and bill nodes indicate party and policy area for the respective node type. A cursory view of this graph would suggest that while there is some cross-party collaboration, the bulk of it is expected to occur within parties — a pattern that could be taken as evidence of polarization in the collaboration network.

Yet, *the same* unipartite representation can be derived from two disparate bipartite network structures. Indeed, projecting the networks in panels (b) and (c) at the bottom of Figure 1 using sums over shared cosponsorships results in exactly the same weighted network depicted in panel (a), despite representing two

---

suggesting less heterogeneity in behavior. See Section ?? of the Online SI for details.

*fundamentally different* legislative collaboration environments.

In panel (b), legislators are highly productive in terms of legislative output (given by the large number of bills represented by triangular nodes in the graph), and cross-party work is common (as indicated by the relatively large number of gray triangular nodes in the graph). Indeed, the bipartisan vs. within-party cosponsored legislation ratio is 3 to 4, and the average probability that two bill cosponsors selected at random belong to the same party is 0.43.<sup>5</sup> The graph in panel (c), in contrast, tells a different story altogether. Senators in this network are far less productive in terms of individual bills, more unified in terms of within party cosponsorships, and collaborate only once across the aisle through a single, widely cosponsored bill.<sup>6</sup> Likewise, the bipartisan versus within-party cosponsored legislation ratio is much lower — namely, 1 to 2 — and the average probability that two cosponsors of a bill chosen at random are, in turn, copartisans, is about double — namely 0.84.<sup>7</sup>

This substantive differentiation of bipartisan versus polarized behavior is completely obscured in the network in the top of Figure 1, which depicts the result of projecting either of these bipartite graphs using weights that track the number of bills through which connections happen.<sup>8</sup> In this new network among senators, the strength of within-party ties is much higher than that of ties across party lines, and the average probability that a connection is made with a copartisan is thus fairly high — despite how different the probabilities of randomly picking cosponsors of the same party are in the two networks. Overall, then, relevant information about the nature of collaboration can be lost in aggregating over node types.

---

<sup>5</sup>The probability that any two members of the set of cosponsors are copartisans is closely related to measures used in other areas to quantify the strength of diversity and segmentation across groups in a population — including the ethnic fractionalization index and the Herfindahl-Hirschman index. For the network in panel (b) of Figure 1, the distribution over these probabilities across bills is bimodal, with similar masses at 0 (for all bills in gray) and 1 (for all other bills).

<sup>6</sup>In formal graph-theoretic terms, the vertex connectivity of network (c) is much smaller than that of network (b), with a cutset of only a single bill cosponsored by all legislators: it would only take removing the only shared bill (gray triangle) to separate the network into two disconnected components.

<sup>7</sup>For the network in this panel, the distribution of these probabilities across bills is also bimodal, but now left-skewed, with masses at 0.5 (for the gray bill in the middle) and 1 (for the remaining two bills).

<sup>8</sup>Some recent work develops bipartite (weighted) projection approaches that at least permit some inferences on network degree heterogeneity, but the main issue of non-injectiveness remains (see, among others, Marrs et al., 2020; Baltakys, 2023).

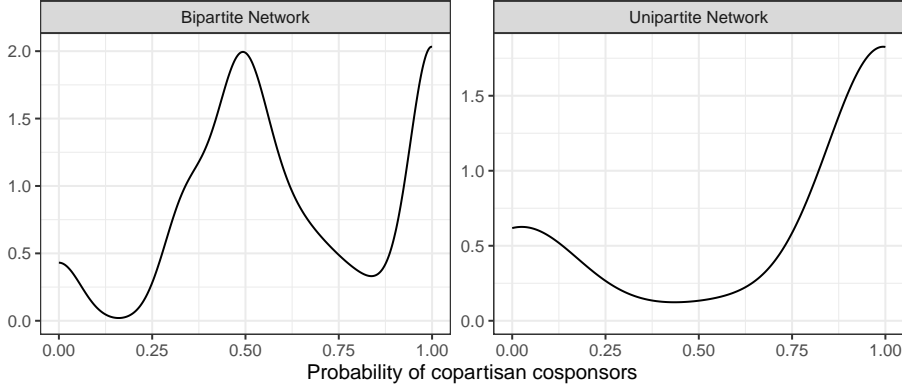


**Figure 3: Probability of copartisan cosponsors during the 107th Senate:** The figure shows the distribution of probabilities that any two distinct cosponsors of a bill belong to the same party (left panel), and the distribution of probabilities that a senator's randomly chosen pair of cosponsors are copartisan (right panel). The former is computed using the full bipartite network of cosponsorships during the 107th Senate, while the latter is computed using the projection onto a weighted unipartite network among senators. The bipartite network (left) shows a good amount of bipartisan cosponsorship whereas the unipartite network (right) shows little such cooperation.

Such aggregation bias is palpable when considering the 107th Senate. Figure 3 shows the distribution of probabilities that a randomly selected pair of cosponsors belong to the same party, computed for each bill in the original bipartite cosponsorship network (left panel) and for each senator in the unipartite senator-only, weighted projection of the bipartite network. When considering the bipartite network, the average probability that a randomly selected pair of each bill's cosponsors belong to the same party is about 0.63. The distribution over these probabilities of copartisan cosponsors is distinctly multimodal, revealing that we are just as likely to find perfectly bipartisan bills (i.e. bills for which the probability of drawing two cosponsors who are also copartisans is about 1/2) as we are to find a perfectly partisan bill (i.e., a bill for which all cosponsors belong to the same party).<sup>9</sup>

The distribution associated with the projected unipartite network, shown on the right panel of Figure 3, paints a completely different picture. Here, the average probability that each senator's randomly selected cosponsor belongs to the same party is about 0.75, suggesting a typical legislator will cosponsor with a set of others who are highly likely to be copartisans.<sup>10</sup> Furthermore, the distribution is markedly skewed left,

<sup>9</sup>To ensure the measure is not distorted by comparing a cosponsor to herself, we compute the bill-specific probability of two copartisan cosponsors being drawn without replacement.

<sup>10</sup>Since we compute a weighted projection, we sample distinct neighbors of a senator in proportion to the strength of their

with a vast majority of senators collaborating mostly with copartisans.

Unfortunately, this kind of strong, artificial clustering present in both the real projected network of the 107th Senate and the simple example in panel (a) of Figure 1 is a manifestation of a more general and systematic phenomenon (Newman, Strogatz, and Watts, 2001; Latapy, Magnien, and Del Vecchio, 2008), and can lead to incorrect conclusions about the extent and nature of polarization in Congress, as we show in Section 4 below.

### **2.3 Motivation for the proposed methodology**

We argue that any modeling tool that hopes to produce plausible answers to the puzzle of productivity and collaboration in times of nominal partisan division should allow researchers to explore the heterogeneity of both legislator and bill attributes. Much as senators might differentially decide to cosponsor based on their personal characteristics, so too might legislation attract cosponsorship based on its different content and the specific context in which it is introduced. A useful model of cosponsorships would thus allow the politics of coalition formation around certain types of legislation to account for this heterogeneity.

Furthermore, it is important for such a model to capture how the interaction of different bill and senator types can lead to cosponsorship collaborations beyond what would be expected from understanding the coalitional dynamics that drive much of legislative politics. The extant literature has identified two substantial predictors of cosponsorship decision that are defined at the senator-bill dyad level, and that result in the kind of non-coalitional homophily and heterophily that is common in social networks of different kinds.

First, individual senators often trade favors with one another, such that cosponsorship may result from quid pro quo behavior and norms of individual reciprocity — *you cosponsored my bill before, I'll cosponsor yours now* (Brandenberger, 2018; Harbridge-Yong, Volden, and Wiseman, 2023). Similarly, scholars have increasingly stressed the role of Senate committees in forming support around legislation, finding evidence that sitting in a committee involved in the life cycle of a bill can affect a legislator's support for it (Porter et al., 2005; Cirone and Van Coppenolle, 2018). Accordingly, a model that aims to capture the full set of forces behind a bipartite network such as that formed by cosponsorships should account for these kinds of connections to the later.

naturally dyadic features that complement group-based drivers of edge formation.

To accommodate these and other theoretical and practical desiderata, we develop `biMMSBM` — a novel and practical alternative to current modeling strategies aiming to predict and explain the edge formation process of bipartite networks. We now turn to the details of our proposed modeling approach.

### 3 The Proposed Methodology

In this section, we begin by describing the core intuition behind the model, which we refer to as the bipartite mixed-membership stochastic blockmodel (`biMMSBM`). We then formally present the full modeling approach, and discuss estimation strategies that enable the analysis of large networks.

#### 3.1 Modeling strategy

We represent an observed network as a bipartite graph, for which there exist two disjoint sets or families of nodes. For a bipartite graph, a set of undirected edges are formed between pairs of nodes belonging to these two different families. In other words, no edge exists between any two nodes of the same family. In our application, senators and legislative bills correspond to these two families. The edges represent cosponsorship relationships, which only occur between senators and bills and do not exist directly among legislators or bills.

The bipartite mixed-membership stochastic blockmodel (`biMMSBM`) assumes that a node belongs to one of several latent groups when interacting with nodes of the other family. For any dyadic relationship between two nodes of different families, the latent group memberships of the nodes determine the likelihood of forming an edge. Thus, a senator may belong to different latent communities when deciding whether to co-sponsor different legislation. Similarly, bills can be sorted into separate latent groups across senator-bill dyads. For instance, John McCain (R-AZ) might have behaved similarly to other Republicans when deciding whether to cosponsor bills related to national security, but might have acted differently when considering bills related to campaign finance reform — a pattern that could help us understand his reputation as a party maverick.

To capture this, we define a probabilistic model to account for the variety of these latent community

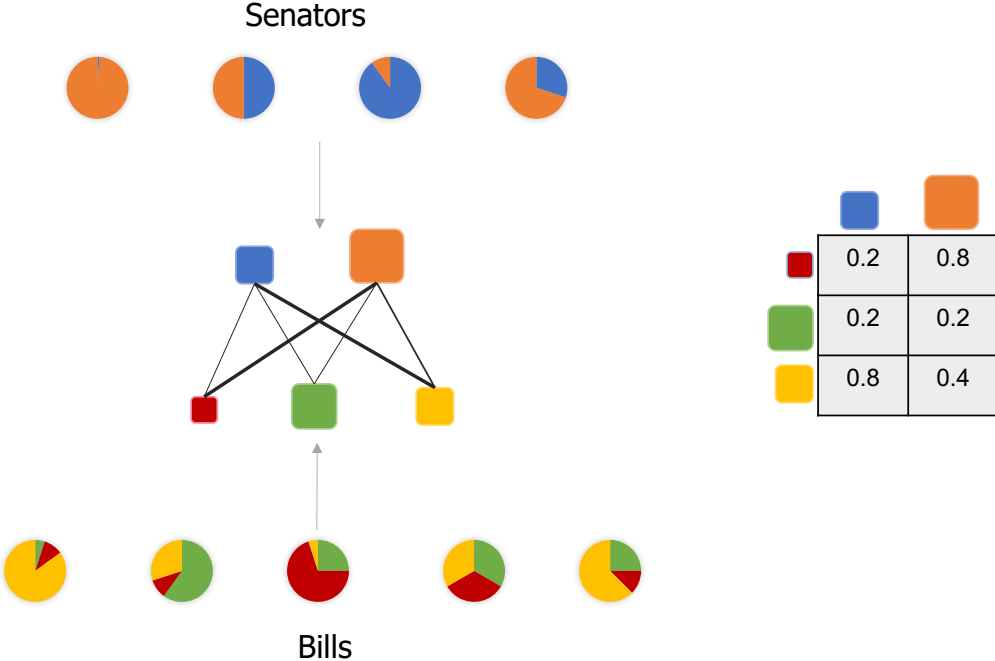


Figure 4: **Schematic representation of the mixed-membership stochastic blockmodel for bipartite networks.** The example above presents a two-by-three latent community setting, whereby four senators have mixed memberships in two communities (blue and orange) while five bills have them for three (yellow, red, green). The senator communities and bill communities themselves have different affinities towards one another, encoded in the block model matrix on the right, which can be represented using the thickness of edges in the graph on the left.

memberships. Figure 4 presents a schematic representation of our model, where different colors in piecharts represent the relative likelihoods of four senators belonging to two different communities (blue and orange). The same idea applies to bills, which might attract different sets of communities of senators as cosponsors. Here, each of five bills belongs to a mixture of three different communities (represented by red, green, and yellow). The fact that each node belongs to their corresponding communities corresponds to the “mixed-membership” portion of the model. Mixed-memberships can be explained using node-level covariates — characteristics of senators and bills, such as ideology for senators and policy area for bills.

The  $2 \times 3$  matrix on the right of Figure 4, represents the so-called *blockmodel*, encoding the probabilities of forming an edge (i.e., cosponsorship) between communities of senators and communities of bills. Some pairs of communities have a higher probability of cosponsorship (e.g., orange group of senators and red group of bills) than others (e.g., blue group of senators and green group of bills). The blockmodel can thus capture a variety of coalitional strategies among senators, affording them flexibility in the way they relate

to different classes of legislation.

Cosponsorship networks are particularly likely to display this kind of stochastic equivalence undergirding our model, as *coalitions* of senators can be expected to support similar *classes* of legislation (e.g. Bratton and Rouse, 2011). The same group-based dynamics, however, are common in other networks — such as those defined by economic trade between countries and co-occurrence of words in documents. We now turn to a formal presentation of the details of our full model.

### 3.2 The Bipartite Mixed-Membership Stochastic Blockmodel

Formally, let  $G(V_1, V_2, E)$  represent a bipartite graph where  $V_1$  and  $V_2$  denote the two disjoint families of nodes ( $V_1 \cap V_2 = \emptyset$ ), and  $E$  represents the set of undirected edges, or pairs of nodes of different families. Suppose that family 1 has a total of  $N_1 = |V_1|$  nodes, and that the number of nodes in family 2 is  $N_2 = |V_2|$ . For each dyad, we let  $z_{pq} \in \{1, \dots, K_1\}$  denote the latent group, to which node  $p \in V_1$  of family 1 belongs when interacting with node  $q \in V_2$  of family 2, whose latent group membership is denoted by  $u_{pq} \in \{1, \dots, K_2\}$ . In general, we allow  $K_1 \neq K_2$ . Further, we use  $y_{pq} = 1$  to denote the existence of an edge between these two nodes  $\{p, q\} \in E$  while  $y_{pq} = 0$  indicates its absence.

We assume that the probability of edge formation is a function of dyadic predictors  $\mathbf{d}_{pq}$  and a block-model  $\mathbf{B}$ , which is a  $K_1 \times K_2$  matrix representing the log odds of forming an edge between any two latent group members, as illustrated on the right of Figure 4,

$$y_{pq} \mid z_{pq}, u_{pq}, \mathbf{B}, \boldsymbol{\gamma} \stackrel{\text{indep.}}{\sim} \text{Bernoulli} \left( \text{logit}^{-1}(B_{z_{pq}, u_{pq}} + \mathbf{d}_{pq}^\top \boldsymbol{\gamma}) \right), \quad (1)$$

where  $\boldsymbol{\gamma}$  denotes a vector of dyad-level regression coefficients. By including a set of dyadic predictors, the model allows edge formation probabilities to be different even for pairs of nodes that have instantiated the same latent groups, thus relaxing the common assumption of stochastic equivalence made by stochastic blockmodels (or SBMs). Substantively, this allows for scenarios where senator-bill dyads whose respective nodes sort into the same pairs of latent communities to be further differentiated in cosponsorship likelihood by characteristics pertinent to their particular dyad — such as a senator’s collaborative history with the author of a bill.

As is common in mixed-membership SBMs, we define a categorical sampling model for the dyad-specific group memberships,  $z_{pq}$  and  $u_{pq}$ , so that

$$z_{pq} \mid \boldsymbol{\pi}_p \sim \text{Categorical}(\boldsymbol{\pi}_p), \quad u_{pq} \mid \boldsymbol{\psi}_q \sim \text{Categorical}(\boldsymbol{\psi}_q), \quad (2)$$

where the probability that node  $p$  of family 1 (node  $q$  of family 2) belongs to a latent group on any possible interaction is given by  $\boldsymbol{\pi}_p$  ( $\boldsymbol{\psi}_q$ ) — a  $K_1$ -dimensional ( $K_2$ -dimensional) probability vector usually known as the *mixed-membership* vector (represented as the pie charts for each node in Figure 4).

Furthermore, our model incorporates node-level information. This is a critical feature of the model because it incorporates (monadic) senator and bill level predictor information directly into the definition of the mixed-membership probabilities of latent groups. These covariates themselves predict the cosponsorship likelihood through the resulting instantiated element of the blockmodel. Specifically, we assume that the mixed-membership probability vectors are generated by a Dirichlet distribution with concentration parameters that are a function of node covariates,<sup>11</sup>

$$\boldsymbol{\pi}_p \mid \boldsymbol{\beta}_1 \sim \text{Dirichlet} \left( \left\{ \exp(\mathbf{x}_p^\top \boldsymbol{\beta}_{1g}) \right\}_{g=1}^{K_1} \right), \quad \boldsymbol{\psi}_q \mid \boldsymbol{\beta}_2 \sim \text{Dirichlet} \left( \left\{ \exp(\mathbf{w}_q^\top \boldsymbol{\beta}_{2h}) \right\}_{h=1}^{K_2} \right), \quad (3)$$

where hyper-parameter vectors  $\boldsymbol{\beta}_{1g}$  and  $\boldsymbol{\beta}_{2h}$  contain regression coefficients associated with the  $g$ th and  $h$ th groups of vertex families 1 and 2, respectively.

Putting it all together, the full joint distribution of data and latent variables is given by,

$$\begin{aligned} f(\mathbf{Y}, \mathbf{Z}, \mathbf{U}, \boldsymbol{\Pi}, \boldsymbol{\Psi}, \mid \mathbf{B}, \boldsymbol{\beta}, \boldsymbol{\gamma}) &= \prod_{p,q \in V_1 \times V_2} f(y_{pq} \mid z_{pq}, u_{qp}, \mathbf{B}, \boldsymbol{\gamma}) f(z_{pq} \mid \boldsymbol{\pi}_p) f(u_{pq} \mid \boldsymbol{\psi}_q) \\ &\times \prod_{p \in V_1} f(\boldsymbol{\pi}_p \mid \boldsymbol{\beta}_1) \prod_{q \in V_2} f(\boldsymbol{\psi}_q \mid \boldsymbol{\beta}_2). \end{aligned} \quad (4)$$

This specification allows us to more formally describe the potential issues raised by aggregation illustrated informally on Section 2.2. A typical aggregation strategy simply sums the number of connections to a member of family  $V_2$  shared by two members of family  $V_1$ , which can be obtained by defining an aggregated sociomatrix  $\tilde{\mathbf{Y}} = \mathbf{Y} \mathbf{Y}^\top$ . Under this aggregation strategy, and in the absence of dyadic covariates, the

---

<sup>11</sup>A plate diagram of the proposed full model is presented in Section ?? of the Online SI, with plates delineating the monadic and dyadic portions of the data generating process.

model in Equation (4) implies

$$\mathbb{E}[\tilde{\mathbf{Y}}] = \mathbb{E}[\mathbf{Y}\mathbf{Y}^\top] > \boldsymbol{\Pi} \left[ \mathbf{B}\boldsymbol{\Psi}^\top \boldsymbol{\Psi}\mathbf{B}^\top \right] \boldsymbol{\Pi}^\top \quad (5)$$

where  $\boldsymbol{\Pi}$  is a  $N_1 \times K_1$  matrix that stacks mixed memberships  $\pi_p$  for all  $p \in V_1$ , and similarly for  $\boldsymbol{\Psi}$ . The root of the issue is that the bracketed terms in Equation (5) (i.e., the blockmodel and the mixed-memberships of Family  $V_2$ ) are not separately identified from the aggregated sociomatrix  $\tilde{\mathbf{Y}}$ , thus resulting in the kind of observational equivalence illustrated in Figure 1. As a consequence, underlying relationships between members of family 1 can be misconstrued if we rely on the aggregated data to learn about them. Our model prevents this possibility by modeling the original bipartite network directly, without resorting to aggregations or projections.

### 3.3 Estimation

With the thousands of vertices and millions of potential edges involved in an application such as bill cosponsorships, sampling directly from the posterior distribution given in Equation (4) is computationally prohibitive. To obtain estimates of quantities of interest in a reasonable amount of time, we follow the computational strategy of Olivella, Pratt, and Imai (2022) by first marginalizing latent variables and then defining a stochastic variational approximation to the full posterior. We briefly summarize these computational strategies here.

**Marginalization.** At first, and given their high dimensionality, marginalizing out dyad-specific group memberships (i.e.  $\mathbf{Z}$  and  $\mathbf{U}$ ) may seem attractive. Doing so, however, would result in variational updates that cannot be computed in closed-form, as the Dirichlet-distributed mixed-membership vectors are not conjugate with respect to the Bernoulli likelihood we have adopted. Instead, we collapse the full posterior over the mixed-membership vectors (i.e.  $\boldsymbol{\Pi}$  and  $\boldsymbol{\Psi}$ ):

$$\begin{aligned} & f(\mathbf{Y}, \mathbf{Z}, \mathbf{U}, \mid \mathbf{B}, \boldsymbol{\beta}, \boldsymbol{\gamma}) \\ &= \int \int f(\mathbf{Y}, \mathbf{Z}, \mathbf{U}, \boldsymbol{\Pi}, \boldsymbol{\Psi}, \mid \mathbf{B}, \boldsymbol{\beta}, \boldsymbol{\gamma}) \, d\boldsymbol{\Pi} d\boldsymbol{\Psi} \\ &= \prod_{p,q \in V_1 \times V_2} \left[ \theta_{pq, z_{pq}, u_{pq}}^{y_{pq}} (1 - \theta_{pq, z_{pq}, u_{pq}})^{1-y_{pq}} \right] \end{aligned}$$

$$\times \left( \frac{\Gamma(\xi_p)}{\Gamma(\xi_p + N_2)} \prod_{g=1}^{K_1} \frac{\Gamma(\alpha_{pg} + C_{pg})}{\Gamma(\alpha_{pg})} \right) \left( \frac{\Gamma(\xi_q)}{\Gamma(\xi_q + N_1)} \prod_{h=1}^{K_2} \frac{\Gamma(\alpha_{qh} + C_{qh})}{\Gamma(\alpha_{qh})} \right) \right] \quad (6)$$

where  $\Gamma(\cdot)$  is the Gamma function,  $\alpha_{pg} = \exp(\mathbf{x}_p^\top \boldsymbol{\beta}_{1g})$ ,  $\xi_p = \sum_{g=1}^{K_1} \alpha_{pg}$  (and similarly for  $\alpha_{qh}$  and  $\xi_q$ ), and  $C_{pg} = \sum_{q \in V_2} \mathbf{1}(z_{pq} = g)$  is a count statistic representing the number of times node  $p$  instantiates group  $g$  across its interactions with nodes in family 2 (and similarly for  $C_{qh}$ ). Lastly,  $\theta_{pq, z_{pq}, u_{qp}} = \text{logit}^{-1}(B_{z_{pq}, u_{qp}} + \mathbf{d}_{pq}^\top \boldsymbol{\gamma})$  is the probability of a tie between the vertices in dyad  $p, q$ .

**Stochastic Variational Inference.** To improve the scalability of our proposed approach, we adopt two complementary strategies. First, we rely on a mean-field variational approximation to the collapsed posterior in Equation (6) (Blei, Kucukelbir, and McAuliffe, 2017), which first defines a lower bound  $\mathcal{L}(\boldsymbol{\Phi})$  for this collapsed posterior, and then tightens the bound by updating the parameters  $\boldsymbol{\Phi}$  of the approximating distributions by following a strategy similar to that of the EM algorithm. It has been shown that the type of marginalization scheme we implement improves the quality of the variational approximation in related contexts (Teh, Newman, and Welling, 2007).

Second, we rely on stochastic optimization to find the maximum of the lower bound (Hoffman et al., 2013; Foulds et al., 2013; Dulac, Gaussier, and Largeron, 2020). To do so, our algorithm follows, with decreasing step sizes, a noisy estimate of the gradient of  $\mathcal{L}(\boldsymbol{\Phi})$  formed by subsampling dyads in the original network. Provided the schedule of step sizes satisfies the Robbins-Monro conditions, and the gradient estimate is unbiased, the procedure is guaranteed to find a local optimum of the variational target (Hoffman et al., 2013). Critically, it does so while using a fraction of the available data at each iteration, thus dramatically improving estimation time. Details of our exact estimation procedures — including a description of how we compute measures of uncertainty, initialize all relevant parameters and latent variables, and sample dyads to form the sub-network on which gradient estimates are based — are available in Section ?? of the Online Supplementary Information.<sup>12</sup>

---

<sup>12</sup>To support claims about the ability of our model to recover meaningful quantities of interest, our Online SI (Section ??) also contains results of a simulation exercise where we evaluate the performance of our estimation approach with respect to the accuracy of the mixed-membership estimation, the ability of the model’s predictions to reflect structural features of networks it is fit to, the properties of our uncertainty approximation strategy, and exercises demonstrating scalability and estimation time across different

### 3.4 Methodological contributions

While the `biMMSBM` model is an extension of the unipartite MMSBM (Airoldi et al., 2008) and its structural variant (Olivella, Pratt, and Imai, 2022), we believe it makes three methodological contributions. First, while the MMSBM is a popular modeling framework for network data across disciplines, there is no version of it that can be applied to bipartite network data, which are common in political science. The model we propose can take full advantage of information about both kinds of vertices involved in bipartite networks, without the need to aggregate and ignore either. Second, by avoiding projections that are common in practice, our model allows researchers to avoid biased results (such artificially higher clustering) related to either of the types of vertices under study. Finally, and particularly by incorporating node-level predictors, our model allows researchers to make predictions about specific pairs of actors (e.g., which senators will support which specific bills). Such granular predictions are not possible when working with the projected network, which most prior models forced researchers to do.<sup>13</sup>

While alternative existing approaches (such as bipartite versions of the popular ERGM model) could also deliver on these fronts in theory, practice suggests these approaches can be difficult to deploy successfully even in medium-sized data contexts. To explore these issues, we compare the fit of `biMMSBM` to that of a bipartite ERGM fit using the `ergm` package in R on a subset of our data (see Section ?? of the Online SI for the results). This is the only alternative implementation of a model designed to predict edges on bipartite networks that we are aware of. We find that our approach improves upon both classification accuracy and calibration of predicted probabilities while requiring less complex input from users. While `biMMSBM` needs only the number of latent communities for both families as an input, bipartite ERGM requires choosing from a large assortment of potentially relevant sufficient statistics terms.

---

sample sizes.

<sup>13</sup>In addition to these, we also make important contributions to the computational front, providing stable and scalable estimation techniques that address the unique challenges brought about by analyzing bipartite data — including the lower informational content available in it than what is typically available when fitting undirected unipartite MMSBMs.

## 4 Empirical Analysis of the 107th U.S. Senate

Before 2021, the Senate had only been perfectly split three other times — with the 107th being the most recent instance of this rare event in the Senate’s history. Despite this, the 107th Senate was not unusual in terms of its productivity, passing about 17% of the 3,242 pieces of legislation introduced between 2000 and 2002 — close to the average of 22% passage rate during the modern Senate — and adopting major legislation, including the Patriot Act and the so-called No Child Left Behind bill.

In fact, such sustained productivity during times of narrow or non-existent partisan majorities is not uncommon, with many major bipartisan pieces of legislation in U.S. history passing under similar circumstances — including the legislation that made the interstate highway system possible, the National Housing Act of 1954, and the Civil Rights Act of 1957. In all, there were a total of 20,660 instances of cosponsorships where a senator attached his/her name to a piece of legislation during the 107th Senate, with about half of them having at least one cosponsor from each party.

To explore the drivers of collaboration in cosponsorship, we use the proposed `biMMSBM` model to better understand why this session of the Senate remained legislatively active, avoiding the gridlock that many associate with partisan divisions. Our model identifies the important role played by junior, bipartisan power brokers. Specifically, they were able to establish the common ground by supporting low-stakes, non-bidding resolutions and popular social programs. In addition, the model detects the important influences of *quid pro quo* cosponsorship behaviors and senate committee experience on cosponsorship likelihood, confirming prior research on the relevance of these features.

Moreover, as we show at the end of this section, fitting a unipartite version of our model would make it impossible to identify these pathways to collaboration. As we would expect given the descriptive analysis in Section 2.2, the unipartite network model reveals little other than partisanship as the main driver of coalitional politics, making it hard to understand how a perfectly divided legislature was able to remain productive.

## 4.1 Model specification and fit

Our goal, then, is to understand the structural and contextual features that made collaboration possible during the 107th Senate. A rich literature on collaboration in Congress suggests that legislators make cosponsorship decisions based on partisanship, seniority, and personal political history (Bratton and Rouse, 2011; Rippere, 2016b). Accordingly, we include senators' *party affiliation, ideology, seniority* and *gender* in our model as monadic predictors for how senators sort into latent communities.

Harward and Moffett (2010) articulates that senators are more likely to cosponsor bills when they share closer preferences with the *sponsor* of the bill, and when they are more connected to their colleagues. To capture this, we model legislation groups as a function of their corresponding sponsors' *party, ideology, seniority* and *gender* (we remove dyads where senators are the sponsors of bills in question).

Lastly, senators tend to cosponsor bills that cover specific policy domains (Harward and Moffett, 2010) and may choose to opt into bipartisan cosponsorships based on topics covered in the legislative bill (Harbridge, 2015). This inclination cannot be modeled in a senator-only unipartite network, but can be directly accounted for when modeling the bipartite structure. We address this possibility by including the *substantive topic* as a bill-level covariate.<sup>14</sup>

To capture the described shifts in the *temporal context* in which bills are introduced, we also include a bill-level (i.e., monadic) covariate indicating whether a bill was presented in the first phase of the Congress (prior to Jeffords leaving the Republican party), in the second phase (post Jeffords leaving and prior to 9/11) or in the third phase (after 9/11). The temporal context under which a piece of legislation is introduced is an additional example of information that would inevitably be discarded in a projected unipartite analysis of the bipartite network (Kirkland and Gross, 2014).

As we indicated earlier, we also pay close attention to two additional forces that can be expected to

---

<sup>14</sup>We also consider two notable alternative specifications: first, we consider a specification in which no additional predictors are included (i.e., the classic mixed-membership stochastic blockmodel). Second, we fit a model that also includes a dyadic indicator of shared state between a senator cosponsor and the sponsor of a bill. We present the results of both exercises in Section ?? of the Online SI.

affect the likelihood of cosponsorship. First, we aim to capture *reciprocity* behaviors, or favor-trading on the Senate floor (Brandenberger, 2018; Harbridge-Yong, Volden, and Wiseman, 2023). The model therefore includes a dyadic predictor measuring, for each senator-bill dyad, the (log) proportion of times the bill’s sponsor in turn cosponsored proposals introduced by the corresponding senator in the previous Congress. As this proportion of reciprocity is heavily skewed and contains a number of zeros, we use the log transformation of non-zero values and an indicator variable for the cases of zeros.

Second, our dyadic model includes the *number of committees* shared by a senator and a piece of legislation. A greater number of shared committees indicates a higher chance that the senator has overseen the development of a bill and holds relevant substantive expertise. While the roles of committees have been studied previously (Porter et al., 2005; Cirone and Van Coppenolle, 2018), our analysis directly examines how overlap in committees between legislator and legislation relates to cosponsorship. Relatedly, Gross and Kirkland (2019) find evidence of strong predictive power of shared committee *leadership* among the subset of ranking legislators when exploring cosponsorship decisions.

With predictors at the monadic and dyadic levels in place, we determine the number of latent groups for senators and bills. To do this, we first randomly select 25% of data as a test set, and compare models with a range of possible latent group-size pairings through the area under the ROC curve (AUROC) values for the out-of-sample edges. We then select the group sizes offering the best fit according to this criterion, resulting in 3 groups each for legislators and bills, i.e.,  $K_1 = K_2 = 3$ .

To evaluate model performance, we generate a set of 50 replicates of the out-of-sample network from the posterior predictive distribution of our model, and compare the distribution of a number of network-level statistics (e.g., the degree distributions of senators and bills, the family-specific distributions of edge-shared partners and  $k$ -stars, etc.) to the ones observed in our test set. Figure 5 shows the results of this exercise, with black bars covering the interquartile range of each statistic across network replicates, and the red line indicating the corresponding observed value in the test set. The model generally fits the out-of-sample network well, as indicated by the fact most red lines fall inside of their corresponding black bars, capturing structural network features without the need to make them part of the explicit model specification. The

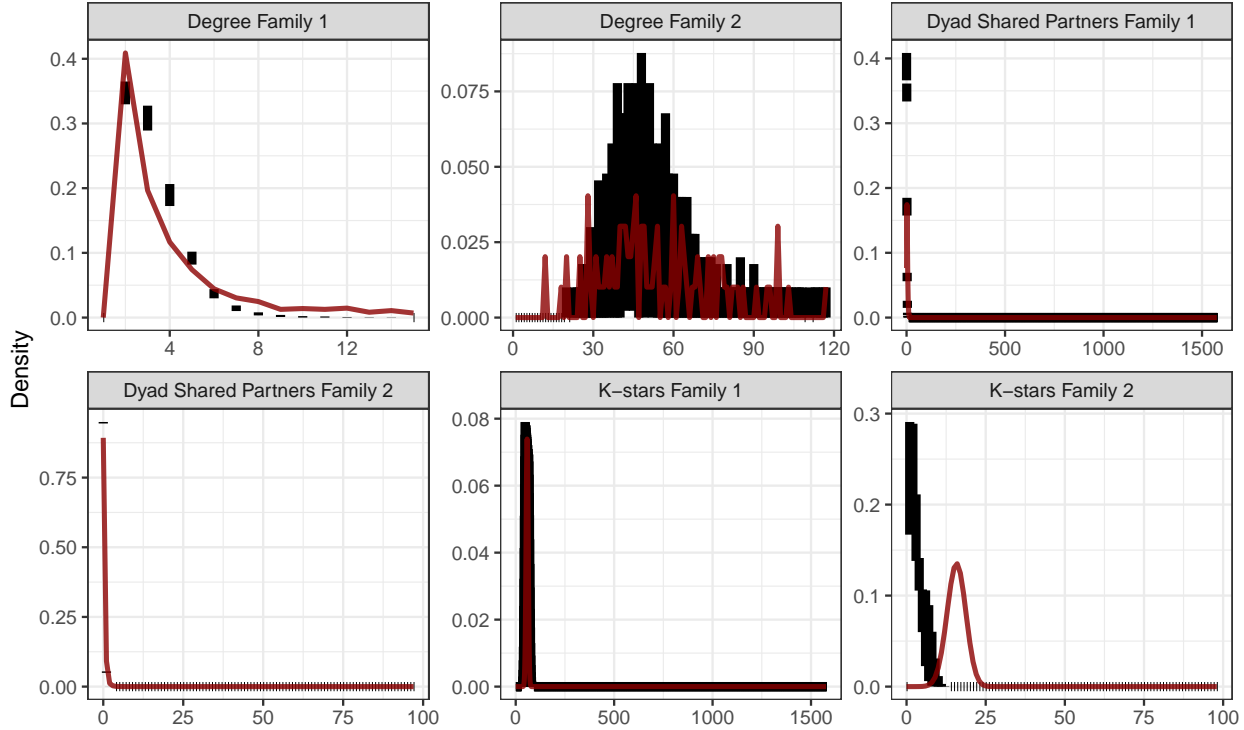


Figure 5: **Posterior predictive goodness-of-fit checks, out-of-sample.** Vertical black rectangles show interquantile range of values obtained across 50 replicate networks. The red line in each panel tracks the value observed in network formed by a random sample of 25% of cosponsorship decisions made during the 107th Senate. Overall, the model does a good a job at replicating structural features of the observed network, as indicated by the overlap between the black bars and the red lines. The number of  $k$ -stars of bills, however, tends to be underpredicted in the out-of-sample set.

exception to this is the distribution over  $k$ -stars among bills, which the model tends to underpredict. The model also exhibits high out-of-sample predictive accuracy and calibration, generating higher predicted probabilities for observed edges (relative to observed non-edges) in the test-set 70% of the time while producing well-calibrated predictions (i.e., while ensuring that about  $x\%$  of observed cases with about an  $x/100$  predicted probability of having an edge do, in fact, have one; see Figure A.1 in the Appendix).

Having established that the model generally fits the data well even out of sample, we obtain the estimates of all parameters and hyper-parameters in Equation (4) for this  $K_1 = K_2 = 3$  model fitted to the entire bipartite cosponsorship network in the 107th Senate. More specifically, we compute various quantities of interest in the form of predicted probabilities of block interactions and block memberships. As our discussion hinges on these derived quantities, we present all estimated values in Tables A.4 and A.5 in the

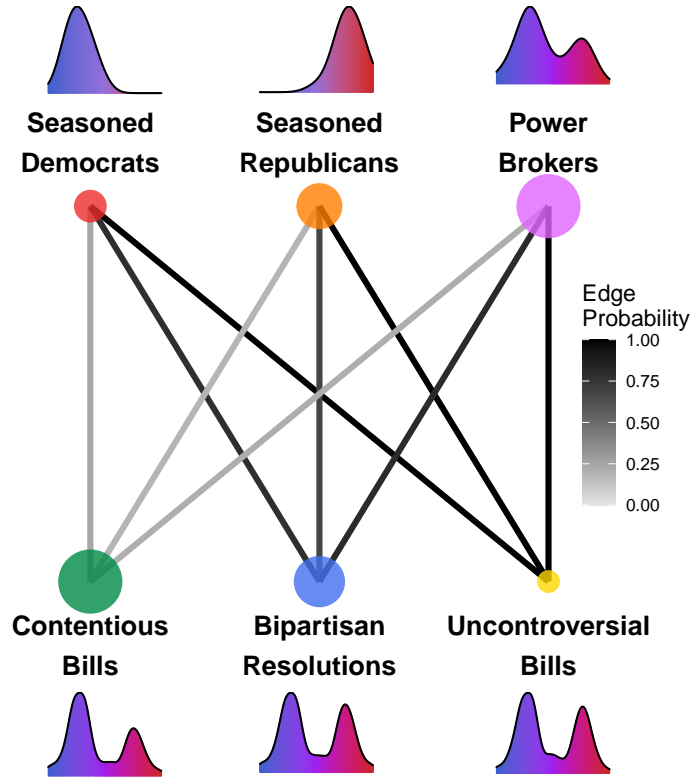


Figure 6: **Blockmodel of senator and legislation latent group connection probabilities.** Block size is proportional to the number of the nodes expected to instantiate the corresponding latent group, and connections between them are shaded to represent the probability that any two members of the corresponding blocks have a cosponsorship tie (darker shades indicate higher probability of a connection). All senator latent groups are likely to connect with a small “Uncontroversial” latent legislation group (comprised of a mix set of resolutions and amendments to social programs by senators from both parties), and least likely to connect with a larger “Contentious” latent group (typically comprised of bills related to new social programs sponsored by women Democrats in the last phase of Congress). Next to each block, we also present a density of ideological positions of member senators (top row) and bill sponsors (bottom row), revealing that while ideology can help distinguish across types of senator coalitions, it cannot discriminate across relevant types of legislation.

Appendix.

## 4.2 Pathways to legislative collaboration

What kinds of coalitions are at play when it comes to making cosponsorship decisions, and how do these coalitions interact when considering different types of legislation? Figure 6 presents the estimated blockmodel for the 107th Senate, showing the likelihood that any two members of a senator and legislation latent group will have a tie between them. Edges in this graph are shaded by the probability that members of senator and bill latent groups have a cosponsorship tie, while nodes are sized proportional to the expected

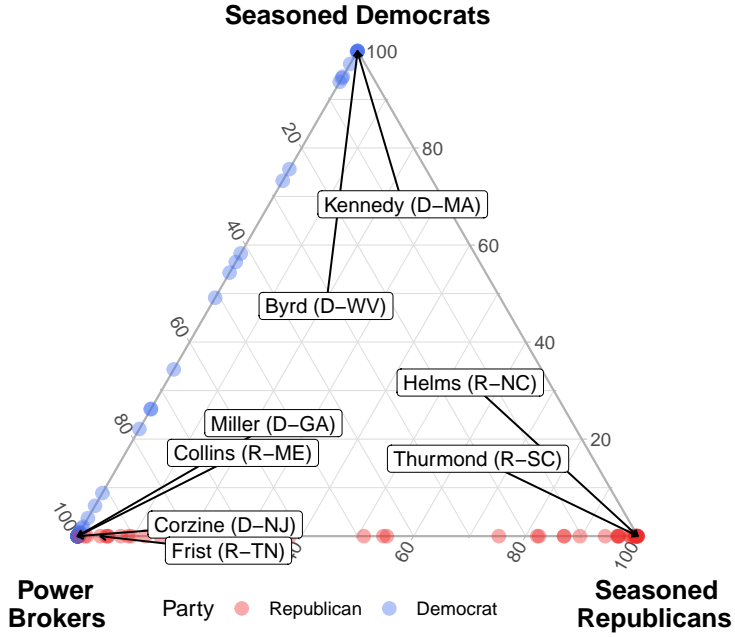


Figure 7: **Ternary plot of senator latent group membership probabilities.** For clarity of presentation, example senators are colored by party. Senators in group 1 (top corner) are more likely to be Democrats, while senators in group 2 (right corner) are more likely to be Republicans; Group 3 (left corner) senators hail from both sides of the aisle and are likely to be junior and involved in cross-partisan bill sharing.

number of times groups are instantiated across dyads. The density for each senator group represents the distribution of ideal points of its members while the density for a bill group is that of its members' sponsors.

As expected, there are estimated senator groups (depicted as the top row of circles in Figure 6) that align well with party memberships. Members of these partisan coalitions include seasoned Republicans (such as Strom Thurmond (R-SC) and Jesse Helms (R-NC)), and seasoned Democrats (like Robert Byrd (D-WV) and Edward Kennedy (D-MA)).

In addition, however, our model identifies a substantial group of senators (depicted in purple) who stand out as having different cosponsorship patterns than their more partisan counterparts. Exemplars of this group, whom we call the *junior power brokers*, include Jon Corzine (D-NJ), Tom Carper (D-DE), Susan Collins (R-ME), Bill Frist (R-TN), Zell Miller (D-GA), and Hillary Clinton (D-NY) — all junior Senators at the time. Figure 7 presents the estimated mixed memberships of all Senators (i.e., their probability of acting as part of any of the discovered latent groups), highlighting a few of the most notable legislators of the session. The top 10 members of each senator latent group by mixed membership probability are presented

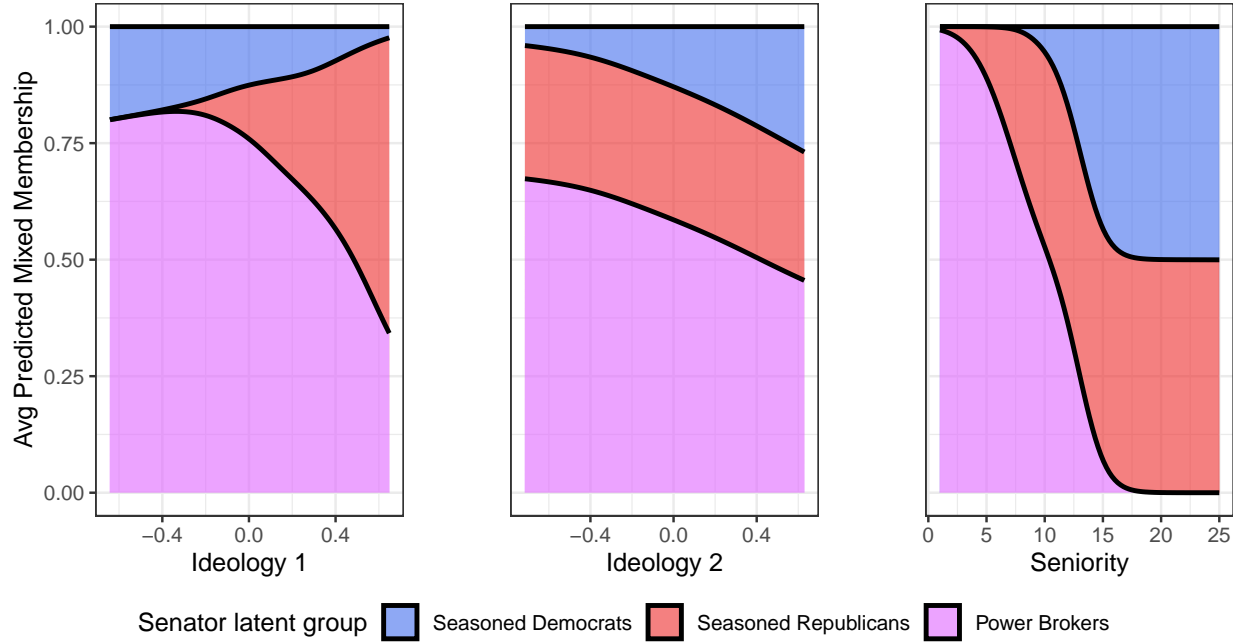


Figure 8: **Predicted Mixed Memberships of senator predictors.** The  $y$ -axes plot average predicted mixed memberships across the three possible senator latent groups, given each shift in value of a senator predictor in the  $x$ -axes; for instance at low values of Ideology (dimension) 1, the average predicted memberships for being in group 1 (Seasoned Democrats) and group 3 (power-brokers) are highest; as Ideology 1 values increase (corresponding to increase in the conservative direction), average predicted group 2 membership (Seasoned Republicans) increases and supplants group 1 entirely.

in Appendix Table A.2.

Indeed, this third bipartisan group is likely to be formed by senators who have little experience in the Senate coming from all over the ideological spectrum, as evidenced by the distribution of ideological positions depicted over the corresponding group in Figure 6.<sup>15</sup> We explore this more directly in the left-most panel of Figure 8, which shows how the probability of group membership changes as a function of ideology. Although the group of junior power brokers (depicted in purple) is primarily predicted to be comprised of left-leaners on the first DW-Nominate dimension, positions along the second ideological dimension (seen in the central panel of Figure 8) — often interpreted as capturing cross-cutting salient issues of the day (Poole and Rosenthal, 2017) — help distinguish this group of senators from their staunch Democratic counterparts.

<sup>15</sup>Plotted quantities are obtained by computing  $\mathbb{E}[\text{SoftMax}(\mathbf{x}_p^\top \hat{\beta}_{1g})]$ , where the expectation is taken over the observed values of all but a focal variable (e.g., ideology), and the  $\hat{\beta}_{1g}$  are estimated monadic coefficients. Full table of estimates of monadic coefficients is in Appendix Table A.5.

Many of these junior power brokers later became new leadership in their respective parties. For example, near the end of the 107th Congress, the Senate Republican Conference saw some leadership changes; importantly, Trent Lott lost substantial support among conservatives and was sharply reprimanded by Democrats over racist remarks he made at Strom Thurman’s 100th birthday. He was forced to step down and was quickly replaced with the much more junior Bill Frist (R-TN), a heart surgeon with a strong platform on healthcare issues and seen as less likely to delve into sticky race issues. Frist is also identified by our model as one of the top members of junior power brokers, ranking among the highest third in terms of probability of instantiating this group when cosponsoring.

Similarly, many of them were pivotal “last” votes in large contentious bills that required just an extra nudge or two for passage. For example, a major bill in the 107th was the *Farm Bill*, designed to repeal the *Freedom to Farm Act* of 1996. While politics over agriculture had historically been regional rather than ideological, the *Freedom to Farm Act* was a significant deviation from that norm. Veteran senators Tom Daschle (D-SD) and Agriculture Committee Chairman Tom Harkin (D-IA) collaborated to bring the bill together, and a series of negotiations began to bring the necessary senatorial support on board — including support for small dairy farmers included in the bill. In the end, the largely Democratic set of supporters was complemented by key support from relatively junior Republicans Susan Collins (R-ME) and Jeff Sessions (R-AL) — again identified by our model as likely members of the power brokers group. This role as brokers is further supported by analyses of the betweenness centrality of Senators who are likely to instantiate this group, which tends to be higher than that of Senators whose membership in the other two groups is more likely (see Table A.6 in the Appendix).<sup>16</sup>

In addition to offering a nuanced view of the collaboration strategies of senators, the model is able to identify the types of legislation which these groups of senators are likely to cosponsor. In this case, the model uncovers three broad classes of bills and resolutions (depicted in the bottom row of circles in Figure 6), and the corresponding probabilities that members of any of the three senator groups will support

---

<sup>16</sup>Betweenness centrality measures, for each node, the number of shortest paths that include it — effectively providing a sense of the extent that a node serves as a “bridge” when connecting any two other nodes in the network, and thus how often nodes can broker relationships in the network.

them through cosponsorship decisions. Critically, while ideology plays an important role in defining the latent senator groups that structure cosponsorship (with right-skewed, left-skewed, and bimodal distributions characterizing membership into the three groups at the top of Figure 6), no such differences in ideology of sponsors can help distinguish across the groups of legislation uncovered by our model (as indicated by the similarly bimodal densities of sponsor ideology across all three groups in the bottom of Figure 6).

We next show that investigating this nuance in bill composition can help us understand how cosponsorship collaborations took place during this nominally partisan session of Congress.

### 4.3 Legislation types that facilitate cosponsorship

The largest type of legislation uncovered by our model is also the least likely to be supported by members of any senator group, suggesting that the bulk of legislation introduced in the Senate received little support from Senators other than the original sponsor. This latent class of bills, which we labeled “Contentious Bills” in Figure 6, consists of high-stakes bills on controversial economic issues and social programs, including those that handle the allocation of public funds for such programs. For example, the *Senior Self-Sufficiency Act* (SN 107 2842), *Bioterrorism Awareness Act* (SN 107 1548), and the *Nationwide Health Tracking Act of 2002* (SN 107 2054) belong to this group. Appendix Table A.3 presents details of legislation with the top ten mixed membership probabilities in each of the three latent groups.<sup>17</sup>

The size of the “Contentious Bills” group grew during the third and last phase of the 107th Senate, after the 9/11 attacks. This is easily seen in Figure 9, which presents radar plots of predicted legislation memberships by phase of the Congress (panels from left to right present bills from the pre-Jeffords’ split phase, post-Jeffords’ split second phase, and post 9/11 phase). Each radar graph positions the six observed substantive topics along spokes of a wheel, and plots the predicted number of bills on that topic as a point along the corresponding spoke: the farther away from the wheel center, the more bills are predicted to be

---

<sup>17</sup>The group is also very likely to contain legislation introduced by junior Democrat women — especially during the last phase of this Senate session. Indeed, for the top one hundred pieces of legislation with highest mixed memberships in this group, all are Democrats, and 96 are female. Although the larger volume of legislation introduced by female Democratic Senators is not surprising (the 107th was also noteworthy for re-invigorating the trend in female membership started in 1992, during the so-called “Year of Woman”), the lack of support elicited by such efforts invites further examination. We leave this for future research.

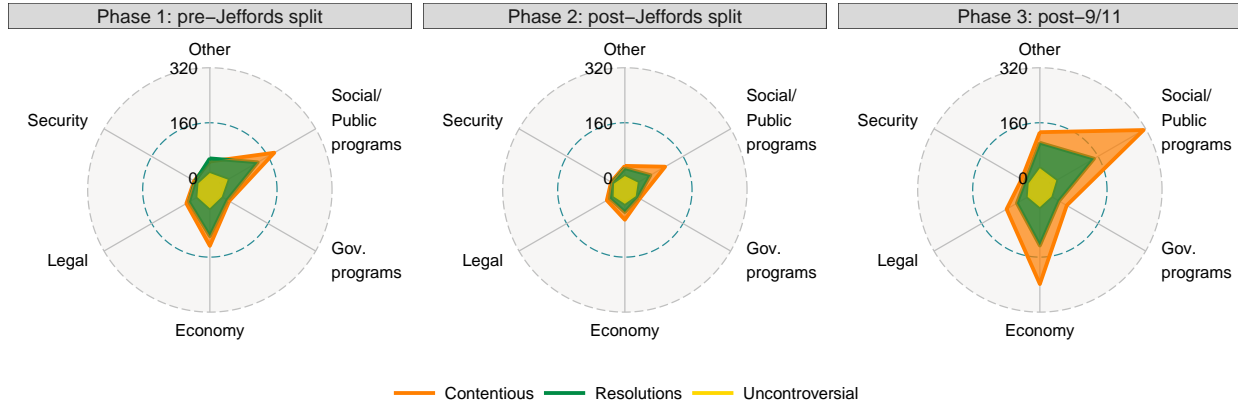


**Figure 9: Radar graphs of predicted legislation by topic within each phase of Congress, by bill latent group.** Panels are phases 1 (pre-Jeffords split), 2 (post-Jeffords split), and 3 (post 9/11) in the Congress, from left to right. Each radar plot includes bill topics as poles, with estimated number of bills in the topic plotted against each pole, by latent group. Phase 2 produces the fewest pieces of legislation, while Phase 3 produces the most. Over time, the predicted number of bills in the “Contentious Bills” group (orange polygon) increases, especially in domains related to social public programs and the economy. The number of bills in the “Bipartisan Resolutions” group grew more slowly than that in the “Contentious Bills” block (green polygon), but has similarly favored social/public programs and the economy. Finally, the number of bills in the “Popular & Uncontroversial” (yellow polygon) changed the least throughout the session.

on that topic. Doing this for each of the three latent groups results in the three shaded polygons presented in each panel of the figure.<sup>18</sup> The dominance of bills in the “Contentious Bills” group in the third phase, depicted in orange, is readily apparent.

How, then, were the different senator groups able to find common ground in order to avoid stalemate? Clues can be gleaned in the definition of the other two latent bill groups uncovered by our model — the groups we have labeled “Bipartisan Resolutions” and “Uncontroversial Bills” in both Figures 6 and 9. The former is particularly illuminating: its topical composition almost mirrors that of the “Contentious Bills” (i.e., it is comprised of pieces of legislation that deal with controversial public social programs and economic issues, as indicated by the similarly-proportioned shapes of green and orange polygons in Figure 9), but it is likely to be comprised of *resolutions* (primarily concurrent and simple), rather than bills — thus offering lower-stakes opportunities for presenting bipartisan positions that do not result in codified law.<sup>19</sup> Such

<sup>18</sup>The vertices of each polygon are obtained by summing each latent group’s estimated mixed membership proportions for a given topic in a single phase — a way to think of *bills in each group allocated towards each topic* — and plotting these against each topic pole’s total number of bills.

<sup>19</sup>Although joint resolutions carry the same weight of bills, in the sense that they could also ultimately become law, many joint resolutions are typically just as symbolic as their concurrent or simple counterparts (e.g., constitutional amendments are extremely

resolutions, often sponsored by more senior senators, offer opportunities to build bridges across partisan divides without incurring the costs associated with creating laws. Table A.3 in the Appendix contains the top pieces of legislation in the group.

In turn, legislation in the comparatively smaller “Uncontroversial” group (shown in yellow in Figures 6 and 9) also draws consistent cosponsorship support from all senator groups, as pieces in it tend to be either uncontroversial resolutions or bills on popular social programs. As a result, such legislation is widely cosponsored by Republicans and Democrats alike. For instance, the Senate joint resolution over the Sept. 11 attacks (SJ 107 22) has the highest mixed membership probability in this group, followed closely by bills such as the *Railroad Retirement and Survivors’ Improvement Act of 2001* (SN 107 697). These legislations form a small but steady core of that supplements low-stakes efforts (such as those in the “Bipartisan Resolutions” block), that can nevertheless result in substantial legislation, such as the *Family Opportunity Act of 2002* (SN 107 321).

The importance of this meaningful cooperation mechanism revealed by the blockmodel is particularly notable, as the model was able to identify it net of two important drivers of cosponsorship likelihood: *quid pro quo* behaviors (represented by dyadic predictors), measured as the coefficient on the (log) proportion of “reciprocity” (*Log Reciprocity*), and the shared committee experience of a given senator-bill dyad (*Shared Committee*). For the former, and given the log transformation, our model suggests that a 1% increase in the reciprocity (i.e., the proportion of times the sponsor of a piece of legislation acted as a cosponsor for a given senator’s bill in the previous Congress) is associated with a roughly 2% increase in the odds of cosponsorship. In the case of the latter, we find that sharing a committee is significantly and positively associated with collaboration, making cosponsorship about 3 times more likely. These results, which are fully explored in Appendix Table A.4, are consistent with previous research on the determinants of legislative collaboration — lending further credence to our general findings.

In sum, Senators appear to have leveraged a mix of low-stakes resolutions over potentially contentious difficult to ratify). Thus, we typically refer to them as “low-stakes” opportunities for bipartisan work. A notable exception is the so-called continuing resolution, which temporarily extend appropriation levels until the corresponding bills are passed. No such continuing resolutions were part of the “Bipartisan Resolutions” group, as they are typically more contentious.

issues and a small but important set of bills for which there was bipartisan support. This enabled them to build cross-partisan bridges and keep the 107th term from devolving into stalemate. Our model identified these novel patterns of cooperation after accounting for other, more traditional forces that have been found to drive collaboration and cosponsorship. Our application offers clues not only about to which kinds of legislators are best positioned to do so, but about which kinds of *legislation* make such collaborations possible. These and similar insights would be lost when analyses aggregate over bills and their characteristics, as we now demonstrate.

#### 4.4 Comparison with the unipartite network model

We conclude our empirical section by comparing the results of our model against those of a unipartite network model. For direct comparison, we use a unipartite (and static) version of our model, known as dynMMSBM (Olivella, Pratt, and Imai, 2022). As discussed in Section 2.2, we project the bipartite network data onto a unipartite weighted network, in which the weight of edges between senators is given by the number of bills they cosponsor together.<sup>20</sup>

For fair comparison, we keep the model specification as similar to the one used in our bipartite network analysis as possible: three latent groups of senators, and the same set of senator-specific covariates. In addition, we use the estimated senator mixed-membership vectors from bIMMSBM as the initial values of the corresponding vectors in the unipartite model. This increases our confidence that any difference in the learned grouping of legislators is a result of the data aggregation process, rather than the differences of model specification and estimation.

Figure 10 presents the main quantities of interest from this comparison: the estimated blockmodel between the three discovered groups of senators in the left panel (i.e., the propensity of members of any of these groups to collaborate with a member of another latent group) and the composition of these groups in the right panel (i.e., the extent to which different senators are likely to be in any of the three groups).

In contrast to the results shown in Figures 6 and 7, the left and right panels of Figure 10 offer a picture of

---

<sup>20</sup>dynMMSBM can accommodate such weighted networks by using a binomial likelihood, where the weights are modeled as “successes” among a number of trials equal to the number of bills two senators could have cosponsored together.

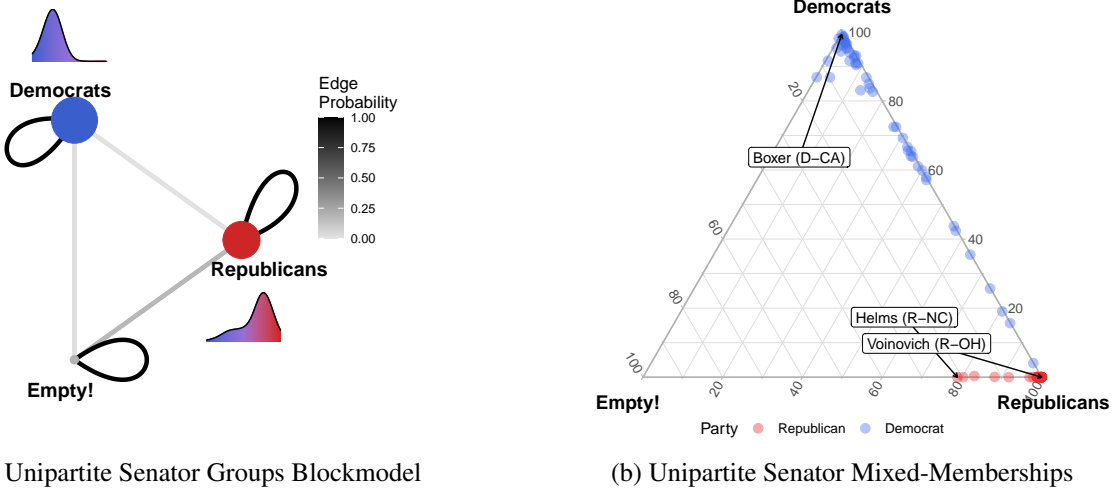


Figure 10: **Results from fitting a MMSBM to the projected cosponsorship network.** After fitting a unipartite MMSBM to the projected cosponsorship network in the 107th Senate, we recover a blockmodel of group interaction probabilities (left panel) and a set of group membership probabilities for Senators (right panel). As expected, the model produces groups that are mostly aligned with partisanship and ideology, as indicated by the ideological distributions of likely members depicted next to each estimated block. We also find evidence of high intra-group collaboration probabilities (especially among Democrats), and very low probabilities of connecting across partisan groups, painting a picture of a highly polarized session.

a polarized, relatively non-cooperative session of Congress, divided clearly along partisan lines — exactly as we expected from our discussion of the issues brought about by the aggregation process involved in projecting a bipartite network onto a unipartite one (see Section 2.2).

While the unipartite model could accommodate three different groups of senators under its specification, the data support membership primarily into two of those latent blocks, leaving the third group essentially empty. Furthermore, membership into these two blocks is strongly aligned with partisanship, as the bulk of Democratic senators (depicted as blue circles on the right panel of Figure 10) concentrate on one vertex of the ternary plot (with liberal Democrat Barbara Boxer being estimated as the senator most likely to instantiate this latent group), while the majority of Republican senators (depicted as red circles) tend to concentrate on another. Those senators who tend to have a minimal likelihood of instantiating the “Empty!” block tend to be Republican ideologues, led by the notoriously conservative Jesse Helms (R-NC).

Moreover, the unipartite model identifies only a moderate amount of collaboration across the aisle, yielding the estimated probability of about .18 that a member of the latent “Democratic” group is connected

in the projected unipartite network to a member of the “Republican” group. In contrast, the probability of a connection between two members of the *same* partisan latent group is estimated to be about .99, as indicated by the darker-shaded loops in the blockmodel on the left of Figure 10. While Democrats enjoyed a slight majority after senator Jeffords decided to leave the Republican party (suggesting that the cohesive majority managed to move legislation along), this picture of polarization painted by the unipartite model gives few clues as to why the 107th Senate was able to remain as productive as it was.

In sum, relying on the projected network of cosponsorships not only misses the rich and nuanced information about legislative collaboration that individual bills have to offer, but it also distorts what we can learn about the nature of legislative coalitions. Using a unipartite model to study naturally bipartite data results in an artificially inflated sense of clustering and group cohesion — a risk that becomes even more pressing when we are interested in group dynamics and polarization that drive processes of network formation.

## 5 Conclusion

We have developed a new approach to modeling bipartite networks that allows researchers to incorporate more complete information available to them rather than projecting these networks onto unipartite networks, leading to biased inference. We extend the mixed-membership network model to two-mode networks with distinct community structures, and incorporate monadic and dyadic predictors into the standard block model specification. Our proposed model therefore allows applied researchers to evaluate hypotheses about affiliation network formation and to make link predictions for previously unobserved dyads.

Our approach offers three main advantages over current alternatives that rely primarily on projections onto unipartite (or one-mode) networks. First, our model makes it possible to explore how characteristics of *both* types of nodes in a bipartite network can contribute to the network formation process in different ways. In the substantive context of legislative studies, this ability to consider the fully disaggregated bipartite network of cosponsorships allowed us to identify the kinds of legislation that allowed members of the 107th Senate to maintain collaborative ties in spite of stark partisan divisions. Specifically, we offer a novel insight on the role played by low-stakes bills and symbolic resolutions on controversial topics in generating the kind

of common ground that can avoid substantial partisan gridlock. Such an insight would have been impossible to unearth by relying on aggregate measures of legislative collaboration.

Second, our model prevents the pathologies in estimation introduced by aggregating over one of the two vertex types in naturally bipartite networks. Such pathologies tend to manifest as artificial network characteristics and aggregation bias — particularly problematic issues when inference about those characteristics is of scientific interest. Substantively, in the case of legislative collaboration through cosponsorship, we showed how analyzing the unipartite projected network of cosponsorships can induce high clustering along partisan lines, thus obscuring the important role some legislators play in generating the kind of bipartisan collaboration that can explain how a perfectly divided Senate like the 107th can remain productive. By relying on our approach, we are able to identify a set of key power brokers (many of whom were junior legislators at the time) who were willing to cross the aisle routinely in search for willing collaborators.

Finally, and by incorporating node-level and dyadic predictors, our approach allows us to evaluate theorized predictors of cosponsorship surrounding the relationship senators might have with the bills themselves. In the case of cosponsorships, we were able to offer further evidence that shows the value of reciprocity norms in legislative collaboration. Relatedly, our model allows researchers to make predictions about which legislators are likely to support a new bill with given characteristics — a much finer level of detail than what an aggregate, legislator-to-legislator framework could afford us. What is more, these types of predictions remain feasible, as they can be thought of as downstream outcomes of the quantities our model allows us to estimate directly.

As bipartite networks are quite common in the social sciences, we see natural applications in a number of different domains. For example, our model could be used to explore questions relating to country-trade product networks, state memberships in organizations, posts on social media platforms and hashtags, or product recommendation systems.

In the future, and given the prevalence of bipartite networks observed over time, fruitful extensions of our proposed approach would allow researchers to incorporate dynamics into the generative model of bipartite network formation(for an extension incorporating dynamics in the unipartite case, see Olivella,

Pratt, and Imai, 2022). Such an extension would make forecasting network ties possible even in the absence of other predictors, and it would enable researchers to use the vast amounts of data available in time-stamped two-mode networks.

Similarly, a further avenue for expanding our work would allow for networks of even larger numbers of node-types — allowing, for instance, the incorporation of lobbying firms into the cosponsorship network, or the study of NGOs, IGOs and countries in the international system. Such multi-mode networks can offer alternative ways of conducting co-clustering of multiple actors who are embedded in common networks, but whose connections are indirect. The prevalence of such types of connections warrants the development of more and better tools to study relational data that do not conform to the traditional single-mode network representation, offering alternatives that do not succumb to aggregation bias.

## References

Agneessens, Filip, Henk Roose, and Hans Waege (2004). “Choices of theatre events: p\* models for affiliation networks with attributes”. *Metodoloski zvezki* 1.2, p. 419.

Airoldi, Edoardo Maria, David M Blei, Stephen E Fienberg, and Eric P Xing (2008). “Mixed membership stochastic blockmodels”. *Journal of machine learning research*.

Anderson, William D, Janet M Box-Steffensmeier, and Valeria Sinclair-Chapman (2003). “The keys to legislative success in the US House of Representatives”. *Legislative Studies Quarterly* 28.3, pp. 357–386.

Arnold, Laura W., Rebecca E. Deen, and Samuel C. Patterson (2000). “Friendship and Votes: The Impact of Interpersonal Ties on Legislative Decision Making”. *State and Local Government Review* 32.2, pp. 142–147.

Baltakys, Kestutis (2023). “Inference of monopartite networks from bipartite systems with different link types”. *Scientific Reports* 13.1, p. 1072.

Battaglini, Marco, Valerio Leone Sciabolazza, and Eleonora Patacchini (2020). “Effectiveness of connected legislators”. *American Journal of Political Science* 64.4, pp. 739–756.

Bernhard, William and Tracy Sulkin (2013a). “Commitment and consequences: Reneging on cosponsorship pledges in the US House”. *Legislative Studies Quarterly* 38.4, pp. 461–487.

— (2013b). “Commitment and consequences: Reneging on cosponsorship pledges in the US House”. *Legislative Studies Quarterly* 38.4, pp. 461–487.

Blei, David M, Alp Kucukelbir, and Jon D McAuliffe (2017). “Variational inference: A review for statisticians”. *Journal of the American statistical Association* 112.518, pp. 859–877.

Brandenberger, Laurence (2018). “Trading favors—Examining the temporal dynamics of reciprocity in congressional collaborations using relational event models”. *Social Networks* 54, pp. 238–253.

Bratton, Kathleen A. and Stella M. Rouse (2011). “Networks in the Legislative Arena: How Group Dynamics Affect Cosponsorship”. *Legislative Studies Quarterly* 36.3, pp. 423–460.

Campbell, James E (1982). “Cosponsoring legislation in the US Congress”. *Legislative Studies Quarterly*, pp. 415–422.

Cao, Xun (2009). “Networks of intergovernmental organizations and convergence in domestic economic policies”. *International Studies Quarterly* 53.4, pp. 1095–1130.

Chatterjee, Sourav and Persi Diaconis (2013). “Estimating and understanding exponential random graph models”. *The Annals of Statistics* 41.5, pp. 2428–2461.

Cirone, Alexandra and Brenda Van Coppenolle (2018). “Cabinets, Committees, and Careers: The Causal Effect of Committee Service”. *The Journal of Politics* 80.3, pp. 948–963.

Desmarais, Bruce A and Skyler J Cranmer (2012). “Statistical inference for valued-edge networks: The generalized exponential random graph model”. *PloS one* 7.1, e30136.

Desmarais, Bruce A, Jeffrey J Harden, and Frederick J Boehmke (2015). “Persistent policy pathways: Inferring diffusion networks in the American states”. *American Political Science Review* 109.2, pp. 392–406.

Desposato, Scott W, Matthew C Kearney, and Brian F Crisp (2011). “Using cosponsorship to estimate ideal points”. *Legislative Studies Quarterly* 36.4, pp. 531–565.

Dulac, Adrien, Eric Gaussier, and Christine Largeron (2020). “Mixed-Membership Stochastic Block Models for Weighted Networks”. In: *Conference on Uncertainty in Artificial Intelligence*. PMLR, pp. 679–688.

Fong, Christian (2020). “Expertise, networks, and interpersonal influence in congress”. *The Journal of Politics* 82.1, pp. 269–284.

Foulds, James, Levi Boyles, Christopher DuBois, Padhraic Smyth, and Max Welling (2013). “Stochastic collapsed variational Bayesian inference for latent Dirichlet allocation”. In: *Proceedings of the 19th ACM SIGKDD international conference on Knowledge discovery and data mining*, pp. 446–454.

Fowler, James H. (2006). “Legislative cosponsorship networks in the US House and Senate”. *Social Networks* 28.4, pp. 454–465.

Frank, Ove and David Strauss (1986). “Markov graphs”. *Journal of the american Statistical association* 81.395, pp. 832–842.

González-Bailón, Sandra and Ning Wang (2016). “Networked discontent: The anatomy of protest campaigns in social media”. *Social networks* 44, pp. 95–104.

Gopalan, Prem K and David M Blei (2013). “Efficient discovery of overlapping communities in massive networks”. *Proceedings of the National Academy of Sciences* 110.36, pp. 14534–14539.

Govaert, Gérard and Mohamed Nadif (2003). “Clustering with block mixture models”. *Pattern Recognition* 36.2, pp. 463–473.

Gross, Justin H. and Justin Kirkland (2019). “Rivals or Allies? A Multilevel Analysis of Cosponsorship within State Delegations in the US Senate”. *Congress & the Presidency* 46.2, pp. 183–213.

Grossmann, Matt and Kurt Pyle (2013). “Lobbying and congressional bill advancement”. *Interest Groups & Advocacy* 2.1, pp. 91–111.

Guillaume, Jean-Loup and Matthieu Latapy (2004). “Bipartite structure of all complex networks”. *Information processing letters* 90.5, pp. 215–221.

Handcock, Mark S, Adrian E Raftery, and Jeremy M Tantrum (2007). “Model-based clustering for social networks”. *Journal of the Royal Statistical Society: Series A (Statistics in Society)* 170.2, pp. 301–354.

Harbridge, Laurel (2015). *Is bipartisanship dead? policy agreement and agenda-setting in the House of Representatives*. OCLC: ocn907082845. New York, NY: Cambridge University Press.

Harbridge-Yong, Laurel, Craig Volden, and Alan E Wiseman (2023). “The bipartisan path to effective law-making”. *The Journal of Politics* 85.3, pp. 1048–1063.

Harward, Brian M. and Kenneth W. Moffett (2010). “The Calculus of Cosponsorship in the U.S. Senate”. *Legislative Studies Quarterly* 35.1, pp. 117–143.

Hoff, Peter D (2021). “Additive and Multiplicative Effects Network Models”. *Statistical science* 36.1, pp. 34–50.

Hoff, Peter D, Adrian E Raftery, and Mark S Handcock (2002). “Latent space approaches to social network analysis”. *Journal of the american Statistical association* 97.460, pp. 1090–1098.

Hoffman, Matthew D, David M Blei, Chong Wang, and John Paisley (2013). “Stochastic variational inference”. *The Journal of Machine Learning Research* 14.1, pp. 1303–1347.

Holman, Mirya R, Anna Mahoney, and Emma Hurler (2022). “Let’s Work Together: Bill Success via Women’s Cosponsorship in US State Legislatures”. *Political Research Quarterly* 75.3, pp. 676–690.

Huang, Zan, Xin Li, and Hsinchun Chen (2005). “Link prediction approach to collaborative filtering”. In: *Proceedings of the 5th ACM/IEEE-CS Joint Conference on Digital Libraries (JCDL’05)*. IEEE, pp. 141–142.

Karrer, Brian and Mark EJ Newman (2011). “Stochastic blockmodels and community structure in networks”. *Physical review E* 83.1, p. 016107.

Kim, In Song and Dmitriy Kunisky (2020). “Mapping Political Communities: A Statistical Analysis of Lobbying Networks in Legislative Politics”. *Political Analysis*, pp. 1–20.

Kim, In Song, Steven Liao, and Kosuke Imai (2020). “Measuring Trade Profile with Granular Product-Level Data”. *American Journal of Political Science* 64.1, pp. 102–117.

Kirkland, Justin H and Justin H Gross (2014). “Measurement and theory in legislative networks: The evolving topology of Congressional collaboration”. *Social networks* 36, pp. 97–109.

Kirkland, Justin H. (2011). “The Relational Determinants of Legislative Outcomes: Strong and Weak Ties Between Legislators”. *The Journal of Politics* 73.3, pp. 887–898.

Koger, Gregory (2003). “Position taking and cosponsorship in the US House”. *Legislative studies quarterly* 28.2, pp. 225–246.

Krutz, Glen S. (2005). “Issues and Institutions: “Winnowing” in the U.S. Congress”. *American Journal of Political Science* 49.2, pp. 313–326.

Lancichinetti, Andrea, M Irmak Sirer, Jane X Wang, Daniel Acuna, Konrad Körding, and Luiós A Nunes Amaral (2015). “High-reproducibility and high-accuracy method for automated topic classification”. *Physical Review X* 5.1, p. 011007.

Larremore, Daniel B., Aaron Clauset, and Abigail Z. Jacobs (2014). “Efficiently inferring community structure in bipartite networks”. *Physical Review E* 90.1, p. 012805.

Larson, Jennifer M (2017). “Networks and interethnic cooperation”. *The Journal of Politics* 79.2, pp. 546–559.

Larson, Jennifer M, Jonathan Nagler, Jonathan Ronen, and Joshua A Tucker (2019). “Social networks and protest participation: Evidence from 130 million Twitter users”. *American Journal of Political Science* 63.3, pp. 690–705.

Latapy, Matthieu, Clémence Magnien, and Nathalie Del Vecchio (2008). “Basic notions for the analysis of large two-mode networks”. *Social networks* 30.1, pp. 31–48.

Lawless, Jennifer L., Sean M. Theriault, and Samantha Guthrie (2018). “Nice Girls? Sex, Collegiality, and Bipartisan Cooperation in the US Congress”. *The Journal of Politics* 80.4, pp. 1268–1282.

Maoz, Zeev, Ranan D Kuperman, Lesley Terris, and Ilan Talmud (2006). “Structural equivalence and international conflict: A social networks analysis”. *Journal of Conflict Resolution* 50.5, pp. 664–689.

Marrs, Frank W, Benjamin W Campbell, Bailey K Fosdick, Skyler J Cranmer, and Tobias Böhmelt (2020). “Inferring influence networks from longitudinal bipartite relational data”. *Journal of Computational and Graphical Statistics* 29.3, pp. 419–431.

Minhas, Shahryar, Peter D Hoff, and Michael D Ward (2019). “Inferential approaches for network analysis: Amen for latent factor models”. *Political Analysis* 27.2, pp. 208–222.

Muraoka, Taishi (2020). “The Cosponsorship Patterns of Reserved Seat Legislators”. *Legislative Studies Quarterly* 45.4, pp. 555–580.

Neal, Zachary (2014a). “The backbone of bipartite projections: Inferring relationships from co-authorship, co-sponsorship, co-attendance and other co-behaviors”. *Social Networks* 39, pp. 84–97.

— (2014b). “The backbone of bipartite projections: Inferring relationships from co-authorship, co-sponsorship, co-attendance and other co-behaviors”. *Social Networks* 39, pp. 84–97.

Neal, Zachary P (2020). “A sign of the times? Weak and strong polarization in the US Congress, 1973–2016”. *Social networks* 60, pp. 103–112.

Newman, Mark EJ, Steven H Strogatz, and Duncan J Watts (2001). “Random graphs with arbitrary degree distributions and their applications”. *Physical review E* 64.2, p. 026118.

Olivella, Santiago, Adeline Lo, Tyler Pratt, and Kosuke Imai (2021). *NetMix: Dynamic Mixed-Membership Network Regression Model*. R package version 0.2.0.9013.

Olivella, Santiago, Tyler Pratt, and Kosuke Imai (2022). “Dynamic Stochastic Blockmodel Regression for Social Networks: Application to International Conflicts”. *Journal of the American Statistical Association* 117.539, pp. 1068–1081.

Peixoto, Tiago P (2014). “Hierarchical block structures and high-resolution model selection in large networks”. *Physical Review X* 4.1, p. 011047.

Platt, John et al. (1999). “Probabilistic outputs for support vector machines and comparisons to regularized likelihood methods”. *Advances in large margin classifiers* 10.3, pp. 61–74.

Poole, Keith T and Howard Rosenthal (2017). *Ideology & congress: A political economic history of roll call voting*. Routledge.

Porter, Mason A., Peter J. Mucha, M. E. J. Newman, and Casey M. Warmbrand (2005). “A network analysis of committees in the U.S. House of Representatives”. *Proceedings of the National Academy of Sciences* 102.20, pp. 7057–7062.

Razaee, Zahra S., Arash A. Amini, and Jingyi Jessica Li (2019). “Matched Bipartite Block Model with Covariates”. *Journal of Machine Learning Research* 20.34, pp. 1–44.

Riker, William H. (1962). *The Theory of Political Coalitions*. New Haven: Yale University Press.

Rippere, Paulina S (2016a). “Polarization reconsidered: Bipartisan cooperation through bill cosponsorship”. *Polity* 48.2, pp. 243–278.

Rippere, Paulina S. (2016b). “Polarization Reconsidered: Bipartisan Cooperation through Bill Cosponsorship”. *Polity* 48.2, pp. 243–278.

Rosenman, Evan TR, Cory McCartan, and Santiago Olivella (2023). “Recalibration of Predicted Probabilities Using the “Logit Shift”: Why Does It Work, and When Can It Be Expected to Work Well?” *Political Analysis* 31.4, pp. 651–661.

Schweinberger, Michael (2011). “Instability, sensitivity, and degeneracy of discrete exponential families”. *Journal of the American Statistical Association* 106.496, pp. 1361–1370.

Skvoretz, John and Katherine Faust (1999). “Logit models for affiliation networks”. *Sociological Methodology* 29.1, pp. 253–280.

Sunstein, Cass (2018). *# Republic: Divided democracy in the age of social media*. Princeton University Press.

Sunstein, Cass R. (2009). *Republic.com 2.0*. Princeton University Press.

Tam Cho, Wendy K. and James H. Fowler (2010). “Legislative Success in a Small World: Social Network Analysis and the Dynamics of Congressional Legislation”. *The Journal of Politics* 72.1, pp. 124–135.

Teh, Yee W., David Newman, and Max Welling (2007). *A Collapsed Variational Bayesian Inference Algorithm for Latent Dirichlet Allocation*. Tech. rep. UC Irvine School of Information and Computer Science.

Wang, Peng, Ken Sharpe, Garry L Robins, and Philippa E Pattison (2009). “Exponential random graph (p\*) models for affiliation networks”. *Social Networks* 31.1, pp. 12–25.

Wasserman, Stanley and Philippa Pattison (1996). “Logit models and logistic regressions for social networks: I. An introduction to Markov graphs and”. *Psychometrika* 61.3, pp. 401–425.

White, Arthur and Thomas Brendan Murphy (2016). “Mixed-membership of experts stochastic block-model”. *Network Science* 4.1, pp. 48–80.

Wilson, Rick K and Cheryl D Young (1997). “Cosponsorship in the US Congress”. *Legislative Studies Quarterly*, pp. 25–43.

Zhang, Yan, Andrew J Friend, Amanda L Traud, Mason A Porter, James H Fowler, and Peter J Mucha (2008). “Community structure in Congressional cosponsorship networks”. *Physica A: Statistical Mechanics and its Applications* 387.7, pp. 1705–1712.

Zhou, Zhixin and Arash A. Amini (2019). “Analysis of spectral clustering algorithms for community detection: the general bipartite setting”. *Journal of Machine Learning Research* 20.47, pp. 1–47.

## A Appendix

### A.1 Projecting Bipartite Networks onto Unipartite Networks is a Common Practice

Table A.1: Applications with naturally bipartite applications in top field journals in 2000s. “Projected” indicates unipartite network considered for empirical application.

Author	Journal	Network; Nodes	Projected
<b>Alliances</b>			
Franzese et al. (2012)	PA	country alliances: countries $\leftrightarrow$ alliance treaties	Yes
Kinne & Bunte (2018)	BJPS	defense cooperation agreements (DCA) network; countries $\leftrightarrow$ DCAs	Yes
<b>Communication</b>			
Aarøe & Peterson (2018)	BJPS	media flows; individuals $\leftrightarrow$ stories	Yes
Boucher & Thies (2019)	JOP	Twitter; Twitter users $\leftrightarrow$ tweets	Yes
Siegel & Badaan (2020)	APSR	Twitter; Twitter users $\leftrightarrow$ tweets	Yes
<b>Conflict</b>			
Rozenas et al. (2019)	PA	conflict & treaty network; actors $\leftrightarrow$ treaties	Yes
Nieman et al. (2021)	JOP	troop placements; major $\leftrightarrow$ minor powers	Yes
<b>Congress &amp; Parliament</b>			
Cho & Fowler (2010)	JOP	legislative cosponsorship; legislators $\leftrightarrow$ bills	Yes
Cranmer & Desmarais (2011)	PA	legislative cosponsorship; legislators $\leftrightarrow$ bills	Yes
Box-Steffensmeier et al. (2018)	AJPS	Dear Colleague letters; legislators $\leftrightarrow$ interest groups	Yes
Zelizer (2019)	APSR	cue taking network; legislators $\leftrightarrow$ bills	Yes
Battaglini et al. (2020)	AJPS	legislative cosponsorship; legislators $\leftrightarrow$ bills	Yes
Kim & Kunisky (2020)	PA	Congressional lobbying; special interest groups $\leftrightarrow$ politicians	No
<b>International organizations</b>			
Martinsen et al. (2020)	BJPS	welfare governance network; bureaucrats $\leftrightarrow$ states	Yes
<b>International political economy</b>			
Bodea & Hicks (2015)	JOP	central bank independence for countries/firms; countries $\leftrightarrow$ investors	Yes
Kim et al. (2019)	AJPS	trade network; countries $\leftrightarrow$ products	Yes
<b>Policies</b>			
Fischer & Sciarini (2016)	JOP	state policy collaboration; political actors $\leftrightarrow$ policies	Yes
Gilardi et al. (2020)	AJPS	policy adoption/issue definition; states $\leftrightarrow$ policies	Yes
<b>Political elites</b>			
Nyhan & Montgomery (2015)	AJPS	campaign consultants; consultants $\leftrightarrow$ candidates	Yes
Pietryka & Debats (2017)	APSR	voters-elite network; voters $\leftrightarrow$ elites	Yes
Weschle (2017)	BJPS	party-societal group network; parties $\leftrightarrow$ societal groups	Yes
Weschle (2018)	APSR	political and social actors; political $\leftrightarrow$ social actors	Yes
Jiang & Zeng (2019)	JOP	elite network; elite (lower) $\leftrightarrow$ elite (upper) politicians	Yes
Box-Steffensmeier et al. (2020)	AJPS	campaign donor list sharing; legislators $\leftrightarrow$ lists	Yes
<b>Village networks</b>			
Larson (2017)	JOP	ethnic cooperation; individuals $\leftrightarrow$ ethnic groups	Yes
Haim, Nanes & Davidson (2021)	JOP	police community connections; police $\leftrightarrow$ citizens	Yes

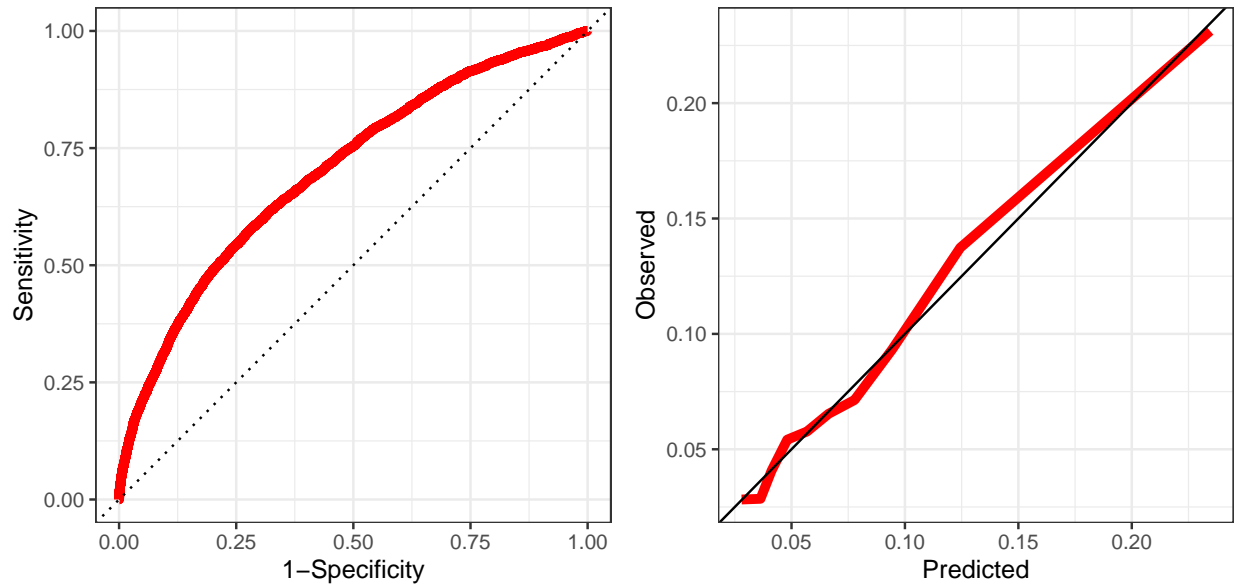


**Figure A.1: Out-of-Sample goodness-of-fit based on edge prediction quality:** The figure shows evidence that our biMMSBM model with  $K_1 = K_2 = 3$  latent groups for each family can adequately predict observed edges in the bipartite cosponsorship network. The left panel shows the Receiver-Operating Characteristic Curve in red, with curves closer to the upper-left corner indicating better predictive accuracy (here, the area under the curve is 0.70, out of a maximum of 1). The right panel shows the calibration of predicted probabilities (after a standard Platt correction) in red, with a curve matching the 45-degree line indicating better predictive calibration.

## A.2 Goodness of Fit

In addition to measures of fit based on overall network statistics, we evaluate fit using two measures of predictive quality: accuracy and calibration. Accuracy is measured using the area under the receiver operating characteristic curve (ROC), and calibration is measured by comparing observed relative frequencies in a test-set to the model’s predicted probabilities.

In Figure A.1, we show the out-of-sample ROC (left panel) as well as the prediction probability calibration plot (right panel).<sup>21</sup> The area under the ROC curve is .7 (with the red curve on the left bending away from the dashed diagonal), and the model’s predictions are well calibrated (with the red curve on the right almost aligning with the solid black diagonal).

<sup>21</sup>We evaluate calibration after applying the standard Platt correction, which fits a logistic regression of observed outcomes on the uncorrected predicted probabilities, and use the transformed scores (Platt et al., 1999; Rosenman, McCartan, and Olivella, 2023).

### A.3 Model outputs

#### A.3.1 Group memberships

Senior Democrats	Senior Republicans	Junior Power Brokers
Byrd, Robert C. [WV]	Helms, Jesse [NC]	Corzine, Jon [NJ]
Inouye, Daniel K. [HI]	Thurmond, Strom [SC]	Carnahan, Jean [MO]
Hollings, Ernest F. [SC]	Lott, Trent [MS]	Carper, Thomas R. [DE]
Kennedy, Edward M. [MA]	Stevens, Ted [AK]	Dayton, Mark [MN]
Breaux, John B. [LA]	Cochran, Thad [MS]	Miller, Zell [GA]
Sarbanes, Paul S. [MD]	Hatch, Orrin G. [UT]	Clinton, Hillary Rodham [NY]
Biden Jr., Joseph R. [DE]	Domenici, Pete V. [NM]	Bayh, Evan [IN]
Baucus, Max [MT]	Grassley, Charles E. [IA]	Nelson, E. Benjamin [NE]
Akaka, Daniel K. [HI]	Smith, Bob [NH]	Stabenow, Debbie [MI]
Leahy, Patrick J. [VT]	Nickles, Don [OK]	Feingold, Russell D. [WI]

Table A.2: **Senators with largest mixed-membership probabilities in each latent group.**

#### A.3.2 Model estimated coefficients

Blockmodel estimates	1 Contentious Bills	2 Bipartisan Resolutions	3 Uncontroversial Bills
1 Democrat	0.2474	0.7844	1.0000
2 Republican	0.1918	0.6765	0.9999
3 Junior Power Brokers	0.2181	0.8095	1.0000
	Coefficient Name	Estimate	SE
<b>Dyadic predictors</b>			
	No reciprocity history	-6.6168	0.1040
	Log proportional reciprocity	2.0015	0.0146
	Shared committee	1.5037	0.0504
<b>Model Summary Statistics</b>			
Lower bound	-591.1986		
Number of dyads	260667		
% Obs. in Each Family 1 Block	0.138	0.285	0.576
% Obs. in Each Family 2 Block	0.578	0.360	0.062

Table A.4: **biMMSBM Estimated Coefficients: blockmodel, dyadic.** Point estimates of coefficients in dyadic regression equation, in the scale of linear predictor, along with their corresponding approximate standard errors. Reciprocity norms and shared committee duties between bill sponsors and potential co-sponsors both increase chances of co-sponsorship.

<b>Contentious Bills</b>	<b>Bipartisan Resolutions</b>	<b>Uncontroversial</b>
SN_107_2842 Senior Self-Sufficiency Act; allocation of \$1M grants to provide supportive services to elderly in noninstitutional residences.	SJ_107_1 Joint resolution proposing amendment to Constitution of US relating to voluntary school prayer.	SJ_107_22 Joint resolution expressing sense of Senate/House regarding terrorist attacks on September 11, 2001.
SN_107_1548 Bioterrorism Awareness Act.	SE_107_82 Resolution authorize production of records by Permanent Subcommittee on Investigations of Committee on Governmental Affairs and representation by Senate Legal Counsel.	SE_107_169 Resolution relative to death of Honorable Mike Mansfield, formerly Senator from Montana.
SN_107_2899 Atchafalaya National Heritage Area Act.	SE_107_9 Resolution notifying Pres. of election of President pro tempore.	SE_107_292 Resolution expressing support for Pledge of Allegiance.
SN_107_3176 Renewal Community Tax Benefit Improvement Act.	SE_107_10 Resolution notifying House of election of President pro tempore.	SE_107_354 Resolution relative to death of Paul Wellstone, Senator from Minnesota.
SN_107_3045 Finger Lakes Initiative Act of 2002.	SE_107_54 Resolution authorizing expenditures by the committees of the Senate.	SE_107_160 Resolution designating Oct 2001, as "Family History Month".
SN_107_1637 Bill to waive limitations in paying costs of projects in response to 9/11.	SE_107_77 Resolution to authorize production of records by Permanent Subcommittee on Investigations of Committee on Governmental affairs.	SE_107_66 Resolution regarding release of 24 US military personnel currently detained by China.
SN_107_2634 225th Anniversary of American Revolution Commemoration Act (establishes educational program).	SE_107_28 Resolution to authorize testimony/legal representation in State of Idaho V. Fredrick Leroy Leas, Sr.	SN_107_321 Family Opportunity Act of 2002.
SN_107_2054 Nationwide Health Tracking Act of 2002.	SE_107_84 Resolution to authorize representation by Senate Legal Counsel in Timothy A. Holt V. Phil Gramm.	SN_107_677 Housing Bond and Credit Modernization and Fairness Act of 2001.
SN_107_1649 Vancouver National Historic Reserve Preservation Act of 2002 (assigns funding).	SC_107_10 Concurrent resolution regarding the Republic of Korea's unlawful bailout of Hyundai Electronics.	SN_107_697 Railroad Retirement and Survivors' Improvement Act of 2001.
SN_107_3092 Children's Health Protection and Eligibility Act of 2002 (authorizes expenditures).	SJ_107_4 Joint resolution proposing amendment to Constitution relating to contributions and expenditures intended to affect elections.	SN_107_1707 Medicare Physician Payment Fairness Act of 2001.

Table A.3: **Bills with largest mixed-membership probabilities in each latent group.**

Group	Coefficient Name	Estimate	SE
<b>Senator predictors</b>			
1 Democrat	Intercept	4.7867	1.3322
	Seniority	0.5993	0.6318
	Ideology 1	-5.5500	1.2965
	Ideology 2	5.0876	1.2912
	Party-Republican	-3.7291	1.3772
	Sex-Male	0.4388	1.2850
2 Republican	Intercept	1.5207	1.4515
	Seniority	0.3924	0.6318
	Ideology 1	10.3447	1.2935
	Ideology 2	-2.2911	1.2906
	Party-Republican	6.1726	1.4587
	Sex-Male	0.8331	1.2850
3 Junior Power Brokers	Intercept	20.3757	1.3299
	Seniority	-0.5417	0.6318
	Ideology 1	-3.3304	1.2916
	Ideology 2	-2.2946	1.2901
	Party-Republican	-0.5346	1.3436
	Sex-Male	-0.0602	1.2847
<b>Bill predictors</b>			
1 Contentious Bills	Intercept	4.2305	0.1224
	Topic:Legal	0.6390	0.1033
	Topic:Social programs Public goods	-0.0517	0.0650
	Topic:Security	0.8542	0.1557
	Topic:Gov operations	0.6023	0.1179
	Topic:Other	-1.5853	0.0729
	Sponsor Seniority	-0.0739	0.0057
	Sponsor Ideology 1	0.6046	0.2433
	Sponsor Ideology 2	-0.2777	0.1449
	Sponsor Party-Republican	-0.6889	0.1783
	Sponsor Sex-Male	-0.4856	0.0842
<b>Bill predictors (continued)</b>			
2 Bipartisan Resolutions	Second Phase	0.8622	0.0789
	Third Phase	0.7629	0.0553
3 Uncontroversial Bills	Intercept	3.3078	0.1226
	Topic:Legal	0.6907	0.1036
	Topic:Social programs Public goods	-0.1533	0.0652
	Topic:Security	0.9016	0.1552
	Topic:Gov operations	0.6219	0.1178
	Topic:Other	-1.1869	0.0731
	Sponsor Seniority	-0.0469	0.0057
	Sponsor Ideology 1	0.3052	0.2438
	Sponsor Ideology 2	-0.0983	0.1457
	Sponsor Party-Republican	-0.1289	0.1786
	Sponsor Sex-Male	-0.2849	0.0842
	Second Phase	0.5371	0.0791
	Third Phase	0.4116	0.0554

Table A.5: **biMMSBM Estimated Coefficients: monadic.** Point estimates of coefficients in the scale of linear predictor, along with their corresponding approximate standard errors.

	Estimate	Std. Error	t value
Baseline: Power Brokers	6401.593	861.9584	7.4268
Senior Democrats	-3009.3133	2112.9178	-1.4242
Senior Republicans	-1447.2995	1568.6299	-0.9227
Multiple $R^2$ : 0.02296	Adjusted $R^2$ : 0.00281	F stat: 1.139	

Table A.6: **Regression of senator between centrality on group assignment probabilities.** Baseline is Group 3, which is positively correlated with between centrality.

# Online Supplementary Information

## A Statistical Model of Bipartite Networks: Application to Cosponsorship in the United States Senate<sup>\*</sup>

Adeline Lo<sup>†</sup> Santiago Olivella<sup>‡</sup> Kosuke Imai<sup>§</sup>

June 2024

---

<sup>\*</sup>The methods described in this paper can be implemented via the open-source statistical software, NetMix, available at <https://CRAN.R-project.org/package=NetMix>. The authors are grateful for comments from Alison Craig, Skyler Cranmer, Sarah Shugars and the participants of the Harvard IQSS Applied Statistics seminar.

<sup>†</sup>Assistant Professor of Political Science, UW-Madison. Email: [aylo@wisc.edu](mailto:aylo@wisc.edu), URL:<https://www.loadline.com/>

<sup>‡</sup>Associate Professor of Political Science, UNC-Chapel Hill. Email: [olivella@unc.edu](mailto:olivella@unc.edu)

<sup>§</sup>Professor, Department of Government and Department of Statistics, Harvard University. 1737 Cambridge Street, Institute for Quantitative Social Science, Cambridge 02138. Email: [imai@harvard.edu](mailto:imai@harvard.edu), URL:<https://imai.fas.harvard.edu/>

## S.1 Additional methodological details

### S.1.1 Plate Diagram of the Proposed Model

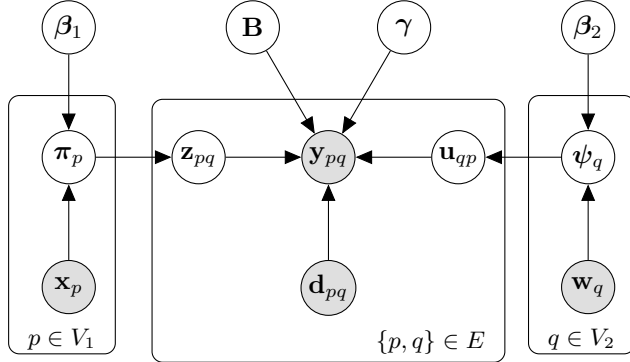


Figure S.1: **Plate diagram of the proposed model.** Observed data represented as shaded nodes; hyperparameters presented as nodes outside plates.

### S.1.2 Details of the Estimation Algorithm

To approximate the collapsed posterior proportional to Equation (6), we first define a factorized distribution of the joint dyad-specific latent group membership variables (i.e.  $\mathbf{Z}$  and  $\mathbf{U}$ ) as follows:

$$m(\mathbf{Z}, \mathbf{U} \mid \Phi) = \prod_{p,q \in V_1 \times V_2} m(z_{pq}, u_{pq} \mid \phi_{pq}) \quad (\text{S.1})$$

where  $\Phi = \{\phi_{pq}\}_{p,q \in V_1 \times V_2}$  are sum-to-one,  $(K_1 \times K_2)$ -dimensional variational parameters.

The goal of variational inference is to find, in the space of functions of the form given by Equation (S.1), one that closely approximates (in KL divergence terms) the target posterior. This is equivalent to maximizing the evidence lower bound  $\mathcal{L}(\Phi)$  to Equation (6) with respect to vectors  $\phi_{pq}$ :

$$\begin{aligned} \hat{\phi}_{pq} &= \underset{\phi_{pq}}{\operatorname{argmax}} \underbrace{\mathbb{E}_m [\log f(\mathbf{Y}, \mathbf{Z}, \mathbf{U}, \mid \mathbf{B}, \boldsymbol{\beta}, \boldsymbol{\gamma})] - \mathbb{E}_m [\log m(\mathbf{Z}, \mathbf{U} \mid \Phi)]}_{\mathcal{L}(\Phi)} \\ &\approx \{(\alpha_{pg} + C'_{pg})(\alpha_{qg} + C'_{qg})(\theta_{pq,g,h}^{y_{pq}}(1 - \theta_{pq,g,h})^{1-y_{pq}})\}_{g,h \in K_1 \times K_2} \end{aligned} \quad (\text{S.2})$$

where  $C'_{pg} = \sum_{q' \in V_2} \sum_{h'=1}^{K_2} \phi_{pq',g,h'}$  is the expected value of the marginal count  $C_{pg}$  under the variational distribution (and similarly for  $C'_{qg}$ ). The approximation in the last line results from using a zeroth-order Taylor series expansion of the expectation in place of calculating the computationally expensive integral over the Poisson-Binomial distribution of the count statistics.

In addition to finding the posterior over mixed-membership vectors, we take an empirical Bayes approach and maximize the lower bound  $\mathcal{L}(\Phi)$  to obtain values of relevant hyper-parameters  $\mathbf{B}$ ,  $\beta$  and  $\gamma$ . After appropriate initialization (see below), then, the full lower bound optimization proceeds iteratively by first updating the variational parameters according to Equation (S.2) (the E-step), and maximizing  $\mathcal{L}(\Phi)$  w.r.t. to the hyper-parameters, holding  $\phi_{pq}$  (and derived global counts  $C_{pg}$  and  $C_{qh}$ ) constant at their most recent value (the M-step), until the change in the lower bound is below a user-specified tolerance. As there are no closed-form solution for these optimal values, we rely on a numerical optimization routine (required gradients are available below). In what follows, we provide details on those steps.

### S.1.2.1 E-step

#### E-step: Z and U

Variational parameters  $\phi_{pq}$  are updated by restricting Equation (S.2) to terms that depend only on  $\mathbf{z}_{pq}$  and  $\mathbf{u}_{pq}$  and taking the logarithm of the resulting expression,

$$\begin{aligned} & \log P(\mathbf{Y}, \mathbf{Z}, \mathbf{U} \mid \mathbf{B}, \beta_1, \beta_2, \gamma, \mathbf{X}_1, \mathbf{X}_2, \mathbf{D}) \\ &= z_{pq,g} \sum_{h=1}^{K_2} u_{qq,h} \{Y_{pq} \log(\theta_{pqgh}) + (1 - Y_{pq}) \log(1 - \theta_{pqgh})\} + \log \Gamma(\alpha_{pg} + C_{pg}) + \text{const.} \end{aligned}$$

Note that  $C_{pg} = C'_{pg} + \mathbb{1}(z_{pq,g} = g)$  and that, for  $x \in \{0, 1\}$ ,  $\Gamma(y+x) = y^x \Gamma(y)$ . As  $\mathbb{1}(z_{pq,g} = g) \in \{0, 1\}$ , we can re-express  $\log \Gamma(\alpha_{pg} + C_{pg}) = z_{pq,g} \log(\alpha_{pg} + C'_{pg}) + \log \Gamma(\alpha_{pg} + C'_{pg})$  and simplify the expression:

$$z_{pq,g} \sum_{h=1}^{K_2} u_{qp,h} \{Y_{pq} \log(\theta_{pqgh}) + (1 - Y_{pq}) \log(1 - \theta_{pqgh})\} + z_{pq,g} \log(\alpha_{pg} + C'_{pg}) + \text{const.}$$

Then take the expectation under the variational distribution  $\tilde{Q}$ :

$$\begin{aligned} & \mathbb{E}_{\tilde{Q}} \{\log P(\mathbf{Y}, \mathbf{Z}, \mathbf{U} \mid \mathbf{B}, \beta_1, \beta_2, \gamma, \mathbf{D}, \mathbf{X}_1, \mathbf{X}_2)\} \\ &= z_{pq,g} \sum_{h=1}^{K_2} \mathbb{E}_{\tilde{Q}}(u_{qp,g}) (Y_{pq} \log(\theta_{pqgh}) + (1 - Y_{pq}) \log(1 - \theta_{pqgh})) + z_{pq,g} \mathbb{E}_{\tilde{Q}} \{\log(\alpha_{pg} + C'_{pg})\} + \text{const.} \end{aligned}$$

The exponential of this corresponds to the (unnormalized) parameter vector of a multinomial distribution  $\tilde{Q}(\mathbf{z}_{pq} \mid \phi_{pq})$ .

The update for  $\mathbf{u}_{qp}$  is similarly derived. Restrict Equation (S.2) to terms that depend only on  $\mathbf{u}_{qp}$  (for specific  $p, q$  nodes in  $V$ ) and taking the logarithm of the resulting expression,

$$\begin{aligned} & \log P(\mathbf{Y}, \mathbf{Z}, \mathbf{U} \mid \mathbf{B}, \boldsymbol{\beta}_1, \boldsymbol{\beta}_2, \boldsymbol{\gamma}, \mathbf{X}_1, \mathbf{X}_2, \mathbf{D}) \\ &= u_{qp,h} \sum_{g=1}^{K_1} z_{pq,g} \{Y_{pq} \log(\theta_{pqgh}) + (1 - Y_{pq}) \log(1 - \theta_{pqgh})\} + \log \Gamma(\alpha_{qh} + C_{qh}) + \text{const.} \end{aligned}$$

Re-express  $\log \Gamma(\alpha_{qh} + C_{qh}) = u_{qp,h} \log(\alpha_{qh} + C'_{qh}) + \log \Gamma(\alpha_{qh} + C'_{qh})$  and simplify the expression:

$$u_{qp,h} \sum_{g=1}^{K_1} z_{pq,g} \{Y_{pq} \log(\theta_{pqgh}) + (1 - Y_{pq}) \log(1 - \theta_{pqgh})\} + u_{qp,h} \log(\alpha_{2qh} + C'_{qh}) + \text{const.}$$

Take the expectation under the variational distribution  $\tilde{Q}$ :

$$\begin{aligned} & \mathbb{E}_{\tilde{Q}} \{\log P(\mathbf{Y}, \mathbf{Z}, \mathbf{U} \mid \mathbf{B}, \boldsymbol{\beta}_1, \boldsymbol{\beta}_2, \boldsymbol{\gamma}, \mathbf{D}, \mathbf{X}_1, \mathbf{X}_2)\} \\ &= u_{qp,h} \sum_{g=1}^{K_1} \mathbb{E}_{\tilde{Q}}(z_{pq,g}) (Y_{pq} \log(\theta_{pqgh}) + (1 - Y_{pq}) \log(1 - \theta_{pqgh})) + u_{qp,h} \mathbb{E}_{\tilde{Q}} \{\log(\alpha_{2qh} + C'_{qh})\} + \text{const.} \end{aligned}$$

### S.1.2.2 M-step

#### Lower Bound

Expression for the lower bound,

$$\begin{aligned} \mathcal{L}(\tilde{Q}) &= \mathbb{E}_{\tilde{Q}} [\log P(\mathbf{Y}, \mathbf{Z}, \mathbf{U} \mid \mathbf{B}, \boldsymbol{\gamma}, \boldsymbol{\beta}_1, \boldsymbol{\beta}_2, \mathbf{X}_1, \mathbf{X}_2, \mathbf{D})] - \mathbb{E}_{\tilde{Q}} [\log \tilde{Q}(\mathbf{Z}, \mathbf{U} \mid \boldsymbol{\Phi})] \\ &= \sum_{p \in V_1} \left[ \log \Gamma(\xi_p) - \log \Gamma(\xi_p + N_2) \right] + \sum_{q \in V_2} \left[ \log \Gamma(\xi_q) - \log \Gamma(\xi_q + N_1) \right] \\ &+ \sum_{p \in V_1} \sum_{g=1}^{K_1} \left[ \mathbb{E}[\log \Gamma(\alpha_{pg} + C_{pg})] - \log \Gamma(\alpha_{pg}) \right] + \sum_{q \in V_2} \sum_{h=1}^{K_2} \left[ \mathbb{E}[\log \Gamma(\alpha_{qh} + C_{qh})] - \log \Gamma(\alpha_{qh}) \right] \\ &+ \sum_{(p,q) \in V_1 \times V_2} \sum_{g=1}^{K_1} \sum_{h=1}^{K_2} \phi_{pq,g} \phi_{pq,h} \{Y_{pq} \log \theta_{pqgh} + (1 - Y_{pq}) \log(1 - \theta_{pqgh})\} \\ &- \sum_{g,h=1}^K \frac{(B_{gh} - \mu_{gh})^2}{2\sigma_{gh}^2} - \sum_{j=1}^{J_d} \frac{(\gamma_j - \mu_\gamma)^2}{2\sigma_\gamma^2} - \sum_{g=1}^{K_1} \sum_{j=1}^{J_{1x}} \frac{(\beta_{1gj} - \mu_{\beta_1})^2}{2\sigma_{\beta_1}^2} - \sum_{h=1}^{K_2} \sum_{j=1}^{J_{2x}} \frac{(\beta_{2hj} - \mu_{\beta_2})^2}{2\sigma_{\beta_2}^2} \\ &- \sum_{(p,q) \in V_t} \sum_{g=1}^{K_1} \sum_{h=1}^{K_2} \{\phi_{pq,g} \log \phi_{pq,g} - \phi_{qp,h} \log(\phi_{qp,h})\} \end{aligned}$$

### M-step 1: update for $\mathbf{B}$

Restricting the lower bound to terms that contain  $B_{gh}$  (blockmodel), we obtain

$$\begin{aligned}\mathcal{L}(\tilde{Q}) = & \sum_{p,q \in E_t} \sum_{g=1}^{K_1} \sum_{h=1}^{K_2} \phi_{pq,g} \phi_{qp,h} \{Y_{pq} \log \theta_{pqgh} + (1 - Y_{pq}) \log(1 - \theta_{pqgh})\} \\ & - \sum_{g,h=1}^K \frac{(B_{gh} - \mu_{gh})^2}{2\sigma_{gh}^2} + \text{const.}\end{aligned}$$

Optimize this lower bound with respect to  $\mathbf{B}_{gh}$  using a gradient-based numerical optimization method. The corresponding gradient is:

$$\frac{\partial \mathcal{L}_{B_{gh}}}{\partial B_{gh}} = \sum_{p,q \in V_1 \times V_2} \phi_{pq,g} \phi_{qp,h} (Y_{pq} - \theta_{pqgh}) - \frac{B_{gh} - \mu_{B_{gh}}}{\sigma_{B_{gh}}^2}$$

### M-step 2: update for $\gamma$

Restricting the lower bound to terms containing  $\gamma$  (dyadic coefficients), and recalling that  $\theta_{pqgh} = [1 + \exp(-B_{gh} - \mathbf{d}_{pqt}\gamma)]^{-1}$ , then:

$$\begin{aligned}\mathcal{L}(\tilde{Q}) = & \sum_{p,q \in V_1 \times V_2} \sum_{g=1}^{K_1} \sum_{h=1}^{K_2} \phi_{pq,g} \phi_{qp,h} \{Y_{pq} \log \theta_{pqgh} + (1 - Y_{pq}) \log(1 - \theta_{pqgh})\} \\ & - \sum_j^{J_d} \frac{(\gamma_j - \mu_\gamma)^2}{2\sigma_\gamma^2} + \text{const.}\end{aligned}$$

To optimize this expression w.r.t.  $\gamma_j$  (the  $j$ th element of the  $\gamma$  vector), we again use a numerical optimization algorithm based on the following gradient,

$$\frac{\partial \mathcal{L}(\tilde{Q})}{\gamma_j} = \sum_{p,q \in V_1 \times V_2} \sum_{g=1}^{K_1} \sum_{h=1}^{K_2} \phi_{pq,g} \phi_{qp,h} d_{pqj} (Y_{pq} - \theta_{pqgh}) - \frac{\gamma_j - \mu_\gamma}{\sigma_\gamma^2}$$

### M-step 3: update for $\beta_1, \beta_2$

Let  $\alpha_{pg} = \exp(\mathbf{x}_1^\top \boldsymbol{\beta}_{1g})$ ,  $\xi_p = \sum_{g=1}^{K_1} \alpha_{pg}$ ,  $\alpha_{qh} = \exp(\mathbf{x}_2^\top \boldsymbol{\beta}_{2h})$ , and  $\xi_q = \sum_{h=1}^{K_2} \alpha_{qh}$ . To find the optimal value of  $\boldsymbol{\beta}_{1g}$ , roll all terms not involving the coefficient vector into a constant:

$$\mathcal{L}(\tilde{Q}) = \sum_{p \in V_1} [\log \Gamma(\xi_{1p}) - \log \Gamma(\xi_p + N_2)]$$

$$\begin{aligned}
& + \sum_{p \in V_1} \sum_{g=1}^{K_1} \left[ \mathbb{E}_{\tilde{Q}_2} [\log \Gamma(\alpha_{pg} + C_{pg})] - \log \Gamma(\alpha_{pg}) \right] \\
& - \sum_{g=1}^{K_1} \sum_{j=1}^{J_{1x}} \frac{(\beta_{1gj} - \mu_{\beta_1})^2}{2\sigma_{\beta_1}^2} + \text{const.}
\end{aligned}$$

No closed form solution exists for an optimum w.r.t.  $\beta_{1gj}$ , but a gradient-based algorithm can be implemented to maximize the above. The corresponding gradient w.r.t. each element of  $\beta_{1g}$  is:

$$\begin{aligned}
\frac{\partial \mathcal{L}(\tilde{Q})}{\partial \beta_{1gj}} = & \sum_{p \in V_1} \alpha_{pg} x_{1pj} \left( \mathbb{E}_{\tilde{Q}_2} [\check{\psi}(\alpha_{pg} + C_{pg})] - \check{\psi}(\alpha_{pg}) \right. \\
& \left. + [\check{\psi}(\xi_{1p}) - \check{\psi}(\xi_{1p} + N_1)] \right) \\
& - \frac{\beta_{1gj} - \mu_{\beta_1}}{\sigma_{\beta_1}^2}
\end{aligned}$$

where  $\check{\psi}(\cdot)$  is the digamma function. Again, we can approximate expectations of non-linear functions of random variables using a zeroth-order Taylor series expansion. The M-step for the regression coefficients of the second family is similarly defined.

### S.1.3 Stochastic variational inference

On the  $t$ th iteration, our algorithm completes the following steps:

1. Sample a subset of dyads  $E^t \subset E$ , with corresponding sets of vertices  $V_1^t = \{p : p, q \in E^t\}$  and

$$V_2^t = \{q : p, q \in E^t\}.$$

2. Update all  $\phi_{pq:p,q \in E^t}$  according to Equation (S.2), and compute a set of intermediate global count statistics (after normalization),

$$\hat{C}_{pg} = \frac{N_2}{|V_2^t|} \sum_{q' \in V_2^t} \sum_{h'=1}^{K_2} \phi_{pq',g,h'}; \quad \hat{C}_{qh} = \frac{N_1}{|V_1^t|} \sum_{p' \in V_1^t} \sum_{g'=1}^{K_1} \phi_{p'q,g',h}$$

weighted to match the amount of information contained in the original network.

3. Update global count statistics matrices using an online average that follows an appropriately decreasing step-size schedule:

$$\mathbf{C}_p^{(t)} = (1 - \rho_{p,t}) \mathbf{C}_p^{(t-1)} + \rho_{p,t} \hat{\mathbf{C}}_p; \quad \mathbf{C}_q^{(t)} = (1 - \rho_{q,t}) \mathbf{C}_q^{(t-1)} + \rho_{q,t} \hat{\mathbf{C}}_q$$

where step-size  $\rho_{p,t} = (\tau + t)^\kappa$  such that  $\tau > 0$  and  $\kappa \in (0.5, 1]$ .

4. Update values of hyper-parameters  $\Lambda = \{\beta, \gamma, \mathbf{B}\}$  by taking an “online” step in the direction of the (noisy) Euclidean gradient of  $\mathcal{L}(\Phi)$  w.r.t  $\Lambda$ :

$$\lambda^{(t)} = \lambda^{(t-1)} + \rho_{\lambda,t} \nabla_{\Lambda} \mathcal{L}^{(t)}(\Phi)$$

with appropriate gradients given in Appendix.

Although different dyad sampling heuristics used for Step 1 can result in unbiased gradient estimates (see Gopalan and Blei, 2013, for a few examples), we follow the scheme proposed by Dulac, Gaussier, and Largeron, 2020, which is both simple to implement and has been found to work well in sparse settings. The procedure is:

1. Sample node  $i$  in  $V$  uniformly at random.
2. Form a set  $s_1 = \{i, j : y_{ij} = 1, \forall j \in V\}$  (i.e., set of all connected dyads involving  $i$ ). Form  $M$  sets  $s_0^m = \{i, j : y_{ij} = 0, \exists j \in V\}$  (i.e., a set of some disconnected dyads involving  $i$ ), where each set is of equal cardinality, and the disconnected dyads are sampled uniformly at random and with replacement.
3. Sample, with equal probability, either  $s_1$  or any of the  $s_0^m$  sets. This set of dyads constitutes a subnetwork.

In our application, we set  $M = 10$  and set  $|s_0^m|$  be  $1/M$  times the number of non-links between  $i$  and every other vertex in the network.

After the algorithm converges, we can recover the mixed-membership vectors by computing their posterior predictive expectations:

$$\hat{\pi}_{pg} = \frac{C_{pg} + \alpha_{pg}}{N_2 + \sum_{g'=1}^{K_1} \alpha_{pg'}}, \quad \hat{\psi}_{qh} = \frac{C_{qh} + \alpha_{qh}}{N_1 + \sum_{h'=1}^{K_2} \alpha_{qh'}}$$

#### S.1.4 Initial values for $\phi$ and $\psi$

Implementation of the model requires defining good starting values for the mixed-membership vectors. While spectral clustering methods offer good starting values for  $\pi$  and  $\psi$  in the unipartite setting, applying

it to non-square affiliation matrices poses interesting challenges. To produce high-quality initial values in a viable amount of time we rely on the co-clustering approach of (Govaert and Nadif, 2003), which estimates a simpler, single-membership SBM using a fast EM algorithm.

### S.1.5 Standard error computation

We obtain measures of uncertainty around regression coefficients  $\beta$  and  $\gamma$  by evaluating the curvature of the lower bound at the estimated optimal values for these hyper-parameters. When considering terms that involve these hyper-parameters, the lower bound reduces to the expected value of the log-posterior taken with respect to the variational distribution  $\tilde{Q}$ . Thus, evaluating the Hessian of the lower bound (and the corresponding covariance matrix of the hyper-parameters) requires evaluating that expectation. Details of the required Hessian are below.

#### S.1.5.1 Hessian for $\gamma$

Restricted to terms that involve  $\gamma$ , the typical element of the required Hessian is given by

$$\frac{\partial^2 \mathcal{L}(\tilde{Q})}{\partial \gamma_j \partial \gamma_{j'}} = \sum_{p,q \in V_1 \times V_2} -d_{pq} d_{pqj'} [\bar{\theta}_{pq}(1 - \bar{\theta}_{pq})] - \sigma_\gamma^{-2} \delta_{jj'}$$

where  $\delta_{jj'}$  is the Kronecker delta function, and the term

$$\bar{\theta}_{pq} = \mathbb{E}_{\tilde{Q}}[\theta_{pq}] = \hat{\phi}_{pq}^\top \hat{\mathbf{B}} \hat{\phi}_{qp} + \mathbf{d}_{pq}^\top \hat{\gamma}$$

is a closed-form solution to the expectation over the variational distribution of the model's parameters.

#### S.1.5.2 Hessian for $\beta_1$ and $\beta_2$

In turn, and focusing on Family 1 coefficients, we can characterize the Hessian of the lower bound w.r.t.  $\beta_1$  with

$$\begin{aligned} \frac{\partial^2 \mathcal{L}(\tilde{Q})}{\partial \beta_{jj'} \partial \beta_{jj'}} &= \sum_{p \in V_1} x_{pj} x_{pj'} \alpha_{pg} \left( \check{\psi}(\xi_p) - \check{\psi}(\alpha_{pg}) + \mathbb{E}_{\tilde{Q}}[\check{\psi}(\alpha_{pg} + C_{pg})] - \check{\psi}(\xi_p + N_2) \right. \\ &\quad \left. + \alpha_{pg} \left( \check{\psi}_1(\xi_{pg}) - \check{\psi}_1(\alpha_{pg}) + \mathbb{E}_{\tilde{Q}}[\check{\psi}_1(\alpha_{pg} + C_{pg})] - \check{\psi}_1(\xi_p + N_2) \right) \right) \\ &\quad - \sigma_{\beta_1}^{-2} \delta_{jj'} \end{aligned}$$

for coefficients in the same group  $g$ , and

$$\frac{\partial^2 \mathcal{L}(\tilde{Q})}{\partial \beta_{gj} \partial \beta_{hj}} = \sum_{p \in V_1} x_{pj} x_{pj} \alpha_{pg} \alpha_{ph} \left( \check{\psi}_1(\xi_p) - \check{\psi}_1(\xi_p + N_2) \right)$$

for coefficients associated with different latent groups  $g$  and  $h$ . As before, we use  $\check{\psi}(\cdot)$  to denote the digamma function, and  $\check{\psi}_1(\cdot)$  to denote the trigamma function.

Unlike the Hessian for  $\gamma$ , there are no closed-form solutions for the expectations involved in these expressions. To approximate them, we take  $S$  samples from the Poisson-Binomial distribution of  $C_{pg}$ ,  $C_{pg}^{(s)}$ ,  $s \in 1, \dots, S$ , and let

$$\mathbb{E}_{\tilde{Q}}[\check{\psi}(\alpha_{pg} + C_{pg})] \approx \frac{1}{S} \sum_s \check{\psi}(\alpha_{pg} + C_{pg}^{(s)}); \quad \mathbb{E}_{\tilde{Q}}[\check{\psi}_1(\alpha_{pg} + C_{pg})] \approx \frac{1}{S} \sum_s \check{\psi}_1(\alpha_{pg} + C_{pg}^{(s)})$$

The Hessian for the coefficients associated with Family 2,  $\beta_2$ , is similarly approximated.

## S.2 Simulation results

**Setup.** We simulate bipartite networks with unbalanced numbers of Senator and Bills nodes under 6 different scenarios, defined by overall network size and difficulty of the mixed-membership learning problem. More specifically, we define small (i.e. 300 total nodes) and large (i.e. 3000 total nodes) networks, each with twice as many Bill nodes as there are Senator nodes. In all instances, we define the edge-generating process according to our model, using  $K_1 = K_2 = 2$  latent groups for each of the node types, a single monadic predictor drawn independently from  $N(0, 1.5)$ , and a single irrelevant dyadic predictor drawn from a standard Normal distribution.

To simulate different levels of estimation difficulty, we vary both the blockmodel and the coefficients associated with the mixed-membership vectors, which are set to be equal across the two node types. In the “easy” scenario, memberships are barely mixed, and there is a clear difference in edge probabilities between different groups of the different node types. In contrast, the “hard” scenario is such that all nodes have a roughly equal probability of instantiating each block, and there is little difference in the probabilities of forming edges between blocks, as given by the blockmodel. The “medium” scenario offers a more realistic, in-between estimation problem. The specific values for scenarios are given in Table S.1.

Scenario Difficulty	Blockmodel	Monadic Coefficients
Easy	$\begin{bmatrix} 0.85 & 0.01 \\ 0.01 & 0.99 \end{bmatrix}$	$\begin{bmatrix} -4.50 & -4.50 \\ 0.00 & 0.00 \end{bmatrix}$
	$\begin{bmatrix} 0.65 & 0.35 \\ 0.20 & 0.75 \end{bmatrix}$	$\begin{bmatrix} 0.05 & 0.75 \\ -0.75 & -1.00 \end{bmatrix}$
Medium	$\begin{bmatrix} 0.65 & 0.40 \\ 0.50 & 0.45 \end{bmatrix}$	$\begin{bmatrix} 0.00 & 0.00 \\ -0.75 & -1.00 \end{bmatrix}$
Hard		

Table S.1: Simulation scenarios, defining various levels of estimation difficulty

**Results.** We begin by evaluating the accuracy of mixed-membership estimation by comparing true and estimated mixed-membership vectors (after re-labeling the latter to match the known, simulated group labels using the Hungarian algorithm). Correlations across node types and difficulty scenarios are demonstrated in Figure S.2. Overall, our model retrieves these mixed-membership vectors with a high degree of accuracy — even in regimes in which block memberships play a small role in the generation of edges, and regardless of whether there is an asymmetry in the number of nodes in each family.

Next, we evaluate the accuracy of estimated node-level and dyadic coefficients by simulating derived quantities of interest based on them, and compare these simulated quantities to their true counterparts, as one would when conducting a goodness-of-fit analysis based on posterior predictive distributions. As is typical in network modeling, these derived quantities are structural features of the network (e.g. Hunter, Goodreau, and Handcock, 2008). Figure S.3 depicts three such features — node degree (by node family), the number of partners shared by each dyad, and the minimum geodesic distance between nodes in the network. In each panel, the red line traces the true distribution of these network statistics, while the black vertical bars track their distribution across 100 network replicates, each generated using the estimated coefficients. If the latter are correctly estimated, network replicates should have characteristics that reflect that on which the estimation is based, and the red line should fall squarely within each vertical black rectangle. Overall,

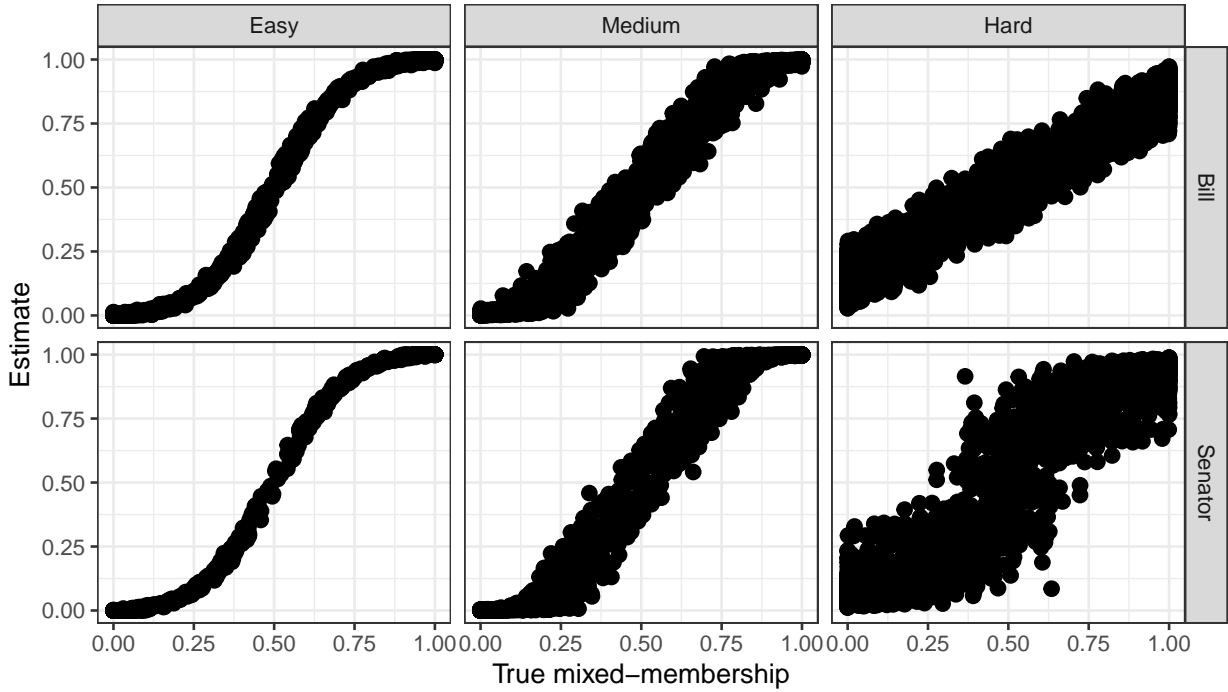
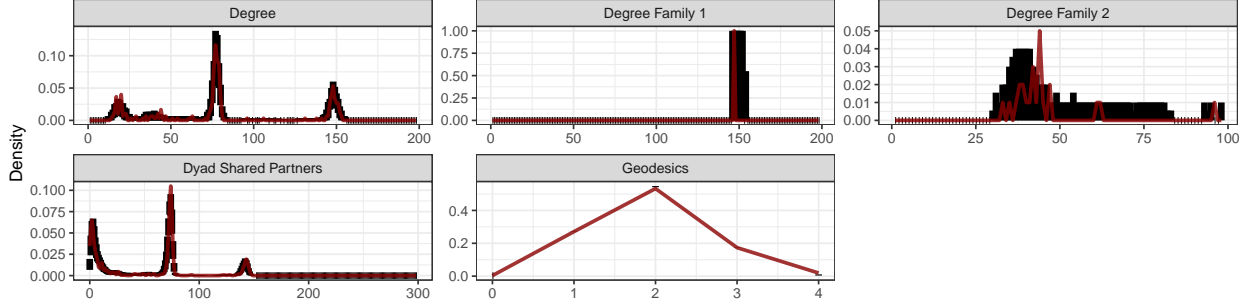


Figure S.2: **Mixed-Membership Recovery**: Estimated and true mixed-membership vectors under the easy, medium, and hard estimation scenarios. In all instances, recovery is excellent.

network characteristics are well recovered by our model, although recovery of the degree distribution for the bill nodes (i.e., the largest family) is less accurate than that of the legislator nodes (i.e., family with fewer vertices).

To evaluate scalability of our approach, we conduct simulations under the “medium” difficulty scenario, as described above. We hold all conditions constant, and increase the total size of the vertex set from 300 to 15,000, keeping twice as many vertices in the largest family as in the smallest family. In all instances, we let the models run until convergence, using the stochastic variational inference procedure described above (in each iteration, we sample 40% of nodes). Models took between 5 seconds and 9 hours to fully estimate, taking anywhere between 100 and 450 iterations to converge. As the time to convergence is affected by the stochastic nature of the estimation, Figure S.4 presents the time per iteration (in seconds) taken to fit our model to networks of different sizes. Overall, although time per iteration increases as the network size grows, even the largest network in our simulation can be reliably fit in under 10 hours on a desktop computer.



**Figure S.3: Posterior Predictive Goodness-Of-Fit:** The figure shows, for a randomly chosen simulated scenario, the extent to which the model can recover structural features of the observed network. The solid red line traces the observed distribution of the different network motifs; solid black rectangles show the central 90% distribution of values observed across 100 network replicates, obtained from the estimated model posterior. A good fit is indicated by lines that always fall within black regions.

Finally, we evaluate the frequentist properties of our estimates of uncertainty in regression parameters by evaluating the extent to which they reflect the variability we can expect from repeated network sampling. To do so, we sample 100 networks from each of our 6 scenarios, for a total of 600 simulated networks. Figure S.5 shows, for each simulation scenario, the difference between our standard errors and the standard deviation across coefficients estimated on each of the network replicates. For small networks, our standard errors can be conservative — particularly for the set of coefficients associated with the smaller group of Senator nodes. As the number of nodes increases, however, our estimated uncertainty more accurately reflects the variability we would expect to see under repeated sampling.

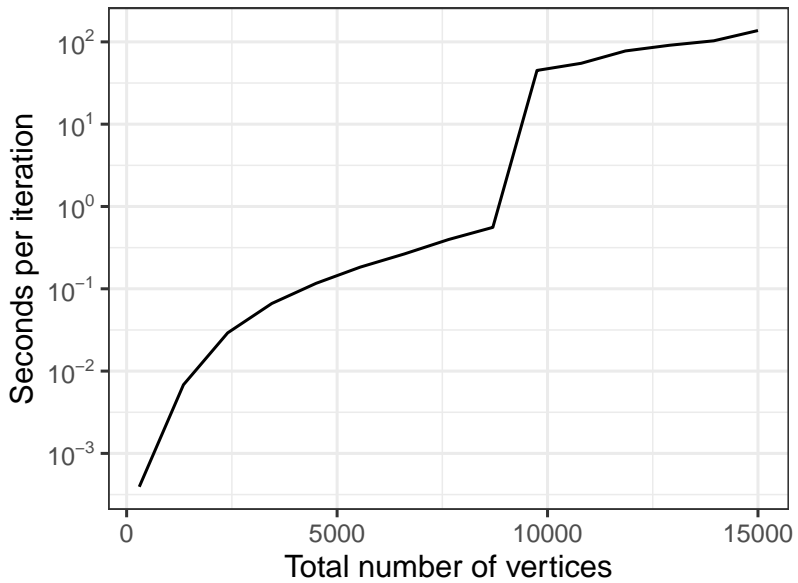


Figure S.4: **Time per iteration for networks of different sizes:** For medium difficulty scenario networks, the plot shows time per iteration (in seconds) taken to fit our model to networks of different sizes.

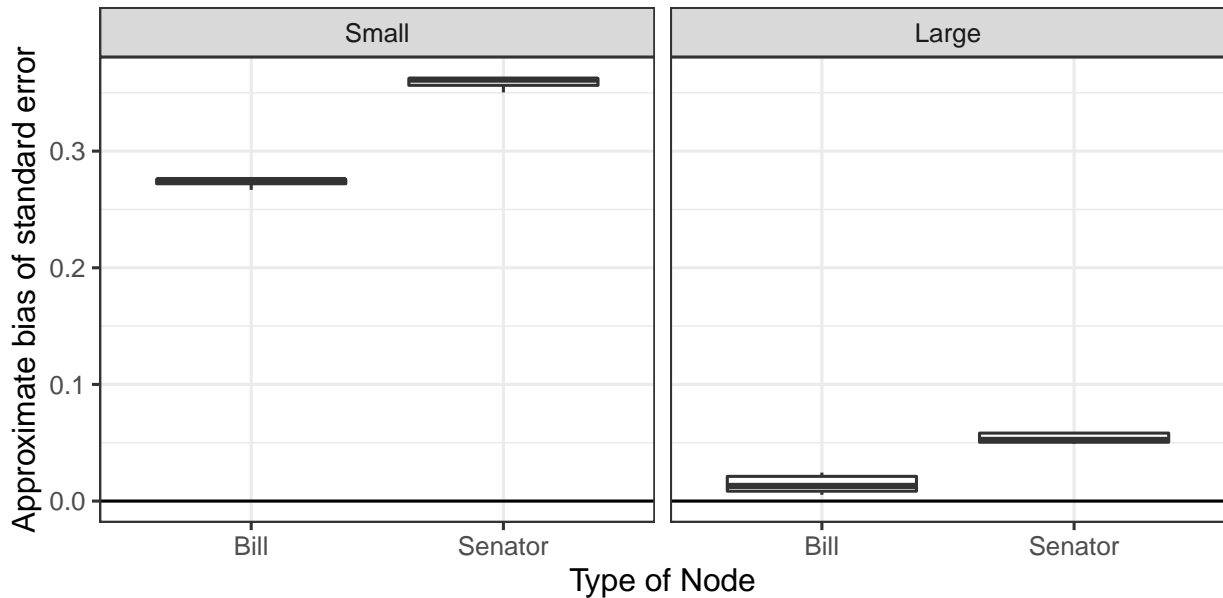


Figure S.5: **Approximate Bias in Standard Errors:** For each simulated network, the figure shows the extent to which our approximate standard errors differ from the standard deviation of coefficients estimated on simulated networks.

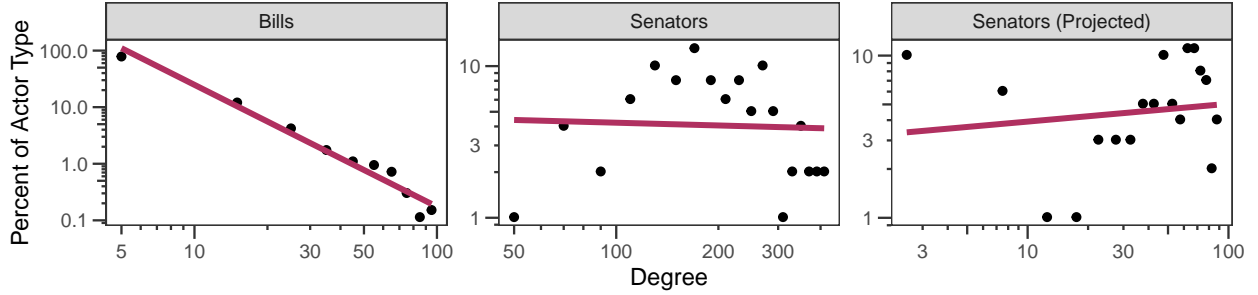


Figure S.6: **Bill and Senator degree distributions.** Degree distributions presented for Bills (left) and Senators (center, in the bipartite network, and right, in the projected network) with a power law distribution overlaid as a red curve (approximated by a linear log-log model). Whereas the power law fits the bill degree distribution quite well, the degree distributions among senators (both in the bipartite graph and in the projected network) differ dramatically from it, illustrating the kind of heterogeneity that can be lost when aggregating over bills in the projection from bipartite to unipartite.

### S.3 Additional empirical results

#### S.3.1 Cosponsorship degree distributions 107th Senate

Figure S.6 presents Senator and Bill degree distributions from the 107th Congress. Bipartite degree distribution calculations differ from unipartite ones in that they are separately conducted for each family, so that senators can display different degree distributions compared to bills. Previous studies of cosponsorship patterns in the U.S. congress have found this to be the case (e.g. Fowler, 2006), and our data reveal similar differences.

Figure S.6 displays a summary of these distributions, plotting the midpoints of the degree histograms for each vertex type. We plot both degrees and their observed relative frequencies (expressed as percentages) in the log scale. When degree distributions follow the common power-law distribution (whereby  $p(x) \propto x^{-\lambda}$  for a given degree  $x$  and  $\lambda > 0$ ) that many other networks exhibit, such log-log plots tend to align with negatively-sloped linear predictions.

This is clearly the case for the degree distribution of bills, depicted on the left panel of Figure S.6. The plot also includes a red line with the predictions of linear log-log model, which shows a good approximation to the pure power-law model if the estimated slope is negative. For bills, the fit of a power-law is almost perfect, indicating that while most bills tend to attract few cosponsors, there is a long and heavy tail of bills

attracting a large number of them. It is precisely this heterogeneity that can result in substantial aggregation bias when projecting the originally bipartite network. It also means that the cosponsorship network is likely to exhibit *scale invariance* for the distribution of bill cosponsors (i.e., we can expect to see a similarly shaped degree distribution if we consider a subset of bills) — justifying the analysis of subnetworks formed by sampling the set of bills (as we do below).<sup>1</sup>

In contrast, the degree distributions of Senators (i.e., the distributions over the number of bills Senators cosponsor) are far from being accurately described by a power-law. This is indicated by the fact that the red line does not fit to the points well on the central and right panels of Figure S.6. Indeed, these distributions are quite different from that of bills, suggesting that there is substantial heterogeneity in the number and strength of connections between senators. This highlights the importance of considering the entire set of senators when studying the structural characteristics of the cosponsorship network, and considering any subset of legislators could result in a misrepresentation of the collaboration network. This difference with respect to the degree distribution of bills also highlights the kind of information that is lost when bills are aggregated over in the process of projecting from bipartite to unipartite networks, as is also evident on the right-most panel of Figure S.6, which appears now to be a mixture of two distributions.

The bipartite network also can accommodate certain types of statistics for descriptive analysis that is not applicable for unipartite networks. They include within-family edge-shared partners and family-specific k-stars. Conversely, several common network statistics for unipartite graphs do not apply in bipartite network settings, such as triangles (bipartite graphs cannot have triangles (Prömel, Schickinger, and Steger, 2002)), or must be adjusted, such as path lengths (which must be even) or minimum degrees (Liu and Ma, 2018). These considerations will play a role when conducting posterior predictive checks of model fit, as they typically rely on evaluating how well a model captures these and other structural features of the modeled network.

---

<sup>1</sup>As pointed out by <empty citation> the distribution also exhibits an interesting deviation from a typical power-law right around the 50 senator mark, indicating the strategic value of having a majority of senators cosponsoring a piece of legislation.

### S.3.2 Model performance comparison

We compare our proposed approach to the most popular, readily available alternative model for bipartite networks: the bipartite ERGM, implemented in the R package `ergm` (Handcock et al., 2023; Hunter, Handcock, et al., 2008; Krivitsky et al., 2023). The bipartite ERGM uses a set of constraints and bipartite-specific network statistics to adapt the canonical, one-model model to bipartite networks. Our goal is to evaluate how well the bipartite ERGM can predict the cosponsorship network of the 107th Senate, using network statistics only. We then compare it to how biMMSBM can fit the same data using only the blockmodel and latent mixed membership vectors.

While we tried fitting the ERGM to the full dataset, we found all of the specifications we tried resulted in failed convergence; the lack of scalability appears to be a major limitation of ERGM. As a result, we focus on a subgraph formed by a random sample of 10% of observed edges. To this subgraph, we fit a model that includes a term for the edge density, the census of 3-stars among senators (i.e., stars involving exactly 1 bill and three senators), a geometrically weighted census of dyad-shared partners among bills (i.e., the distribution over numbers of shared senators for any pair of bills), and geometrically weighted degree distributions for both senators and bills.<sup>2</sup> The latter terms are so-called dyad-dependent terms, and are defined specifically for bipartite networks (Wang, Sharpe, et al., 2009; Wang, Pattison, and Robins, 2013). After fitting the ERGM, all measures of MCMC performance indicated convergence.

For biMMSBM, we use 5 latent communities in each family (a number arrived at by evaluating the AUROC generated by alternative models, as we do in the main analysis. We compare models with 2 – 2, 3 – 3, 3 – 5, and 5 – 5 latent communities).

Figure S.7 offers evidence of better predictive accuracy obtained by biMMSBM on this network, as indicated by a both a higher overall AUROC (0.66 vs. 0.59 obtained by the ERGM; left panel), and far

---

<sup>2</sup>We arrived at this particular specification through *much* trial and error, iterating over specifications that invariably hung or failed to converge. This failure-prone process, often elided from descriptions of empirical exercises that rely on ERGM-type models, is sometimes touted as a feature. Arriving at a specification that works, however, can only offer a weak proof of existence, and even a perfectly specified model can result in an ill-defined probabilistic models (see, for instance, Chatterjee and Diaconis, 2013).

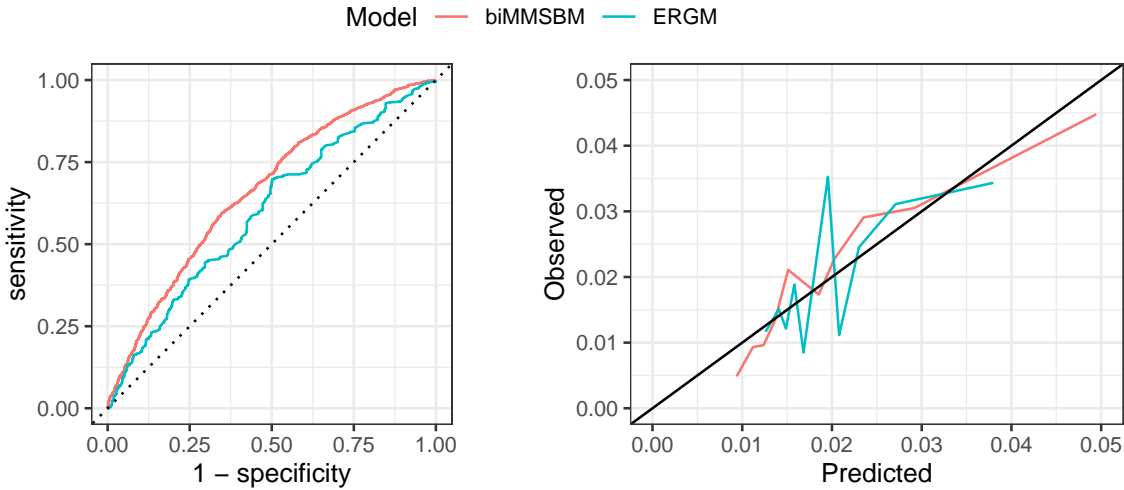


Figure S.7: Measures of predictive accuracy of bipartite ERGM and biMMSBM on subset of cosponsorship network in the 107th Senate. The left panel shows the ROC curves for the ERGM (blue) and biMMSBM (salmon); curves further from the 45-degree reference line indicate better model classification accuracy. The right panel shows the calibration of the same models, with lines closer to the 45-degree line indicating a better match between predicted edge probabilities and observed edge proportions (that is, better calibration). Using both criteria, biMMSBM offers a better predictive fit to the cosponsorship data.

better calibration of predicted probabilities (Platt et al., 1999, after running a Platt correction for both sets of predictions,  $\hat{y}$ ), as indicated by the alignment of the biMMSBM set of predicted probabilities with the corresponding empirical proportions of edges (right panel). These are both in-sample measures of fit, as the fragility of the ERGM estimation prevented us from performing an out-of-sample evaluation.

### S.3.3 Alternative model specifications

**Separating block membership and covariate estimation** Our proposed model allows for joint inference of block membership and predictor effects. It also allows for inclusion of different predictors. To illustrate these possibilities, we restrict the biMMSBM model to infer only block membership or only predictor effects. Findings are briefly summarized below:

1. **Block membership only.** Here no predictors contribute to variation in cosponsorship; instead information is highly concentrated on the block memberships, which are the same for every senator/bill for each respective family of blocks. We find that senators who fall into any of the senator latent groups are likely to have a tie with a bill that instantiates the second bill latent group (ranging 0.613-0.765);

Table S.2: **Only Block Membership Full Model Coefficients.** Coefficient point estimates in linear predictor scale, with corresponding approximate standard errors.

Coefficient	Standard.Error	Blockmodel	Bill 1	Bill 2	Bill 3
<b>Monadic: Senator intercepts</b>		Senator 1 0.0103	0.7649	0.0020	
10.6352	0.4101	Senator 2	0.0122	0.7555	0.0180
6.5183	0.4100	Senator 3	0.0041	0.6130	0.0416
6.0022	0.4097				
<b>Monadic: Bill intercepts</b>					
2.2122	0.0233				
0.0932	0.0235				
1.5949	0.0239				

all other block-to-block interactions are limited (ranging 0.004-0.042). This model suggests low levels of tie formation for bills that fall into any latent group outside of group 2 — a departure from the original joint estimation of results in our main model. The full table of model estimates is shown in Table S.2.

2. **Co-state effects** . In this setting, we incorporate a dyadic predictor for co-state membership between a senator a sponsor of a bill. In this specification, the co-state indicator appears as a strong predictor of a cosponsorship link. Despite this, it is still possible to discern similar results with respect to the discovered groups of legislators and bills. The full table of model estimates is shown in Table S.3.

Table S.3: **Co-State Full Model Coefficients.** Coefficient point estimates in linear predictor scale, with corresponding approximate standard errors.

Group	Coefficient.Name	Estimate	SE	
<b>Dyadic predictors</b>				
	No reciprocity history	-1.5580	0.0196	
	Log proportional reciprocity	0.4354	0.0044	
	Shared committee	0.6560	0.0208	
	Co-state	1.8788	0.0430	
<b>Senator predictors</b>				
1 Democrat	Intercept	9.6722	1.2719	
	Seniority	0.0229	0.3889	
	Ideology 1	-6.7897	1.2818	
	Ideology 2	2.6573	1.2866	
	Party-Republican	-4.8794	1.4720	
	Sex-Male	-0.6568	1.2605	
2 Republican	Intercept	4.2601	1.2716	
	Seniority	0.8223	0.3889	
	Ideology 1	1.7553	1.2792	
	Ideology 2	4.7461	1.2862	
	Party-Republican	1.6111	1.3155	
	Sex-Male	1.0517	1.2606	
3 Junior Power Brokers	Intercept	20.1595	1.2715	
	Seniority	-0.9228	0.3889	
	Ideology 1	-1.0970	1.2781	
	Ideology 2	-7.2593	1.2872	
	Party-Republican	-1.3287	1.3154	
	Sex-Male	-1.1748	1.2605	
<b>Bill predictors</b>				
1 Contentious Bills	Intercept	11.2669	0.1137	
	Topic:Legal	0.8587	0.0303	
	Topic:Social programs Public goods	0.8151	0.0555	
	Topic:Security	0.8096	0.0709	
	Topic:Gov operations	0.5672	0.0675	
	Topic:Other	-5.5515	0.0981	
	Sponsor Seniority	-0.1431	0.0147	
	Sponsor Ideology 1	0.3879	0.5242	
	Sponsor Ideology 2	-0.5291	0.3436	
	Sponsor Party-Republican	-1.3865	0.3804	
	Sponsor Sex-Male	-2.6192	0.1364	
<b>Bill predictors (continued)</b>				
2 Bipartisan Resolutions	Group	Coefficient Name	Estimate	SE
		Second Phase	3.6591	0.6810
		Third Phase	1.9508	0.1370
	Intercept	10.5539	0.1137	
	Topic:Legal	0.7711	0.0308	
	Topic:Social programs Public goods	0.7775	0.0556	
	Topic:Security	1.2102	0.0711	
	Topic:Gov operations	0.9030	0.0678	
	Topic:Other	-4.9057	0.0979	
	Sponsor Seniority	-0.0878	0.0147	
	Sponsor Ideology 1	0.5021	0.5239	
	Sponsor Ideology 2	-0.0069	0.3433	
	Sponsor Party-Republican	-1.6197	0.3802	
	Sponsor Sex-Male	-2.6768	0.1365	
	Second Phase	3.8117	0.6807	
	Third Phase	0.9561	0.1368	
3 Uncontroversial Bills	Intercept	5.5493	0.1362	
	Topic:Legal	1.1332	0.0564	
	Topic:Social programs Public goods	0.7925	0.0676	
	Topic:Security	0.0947	0.1242	
	Topic:Gov operations	0.0754	0.0963	
	Topic:Other	-3.3246	0.0793	
	Sponsor Seniority	-0.0827	0.0166	
	Sponsor Ideology 1	-1.0612	0.5530	
	Sponsor Ideology 2	0.0791	0.3645	
	Sponsor Party-Republican	0.2602	0.4025	
	Sponsor Sex-Male	-1.7541	0.1588	
	Second Phase	1.5149	0.8123	
	Third Phase	-0.0066	0.1424	
<b>Blockmodel</b>				
	Bill 1	Bill 2	Bill 3	
Senator 1	0.3652	0.9819	0.5175	
Senator 2	0.1088	0.1960	0.9918	
Senator 3	0.1399	0.2326	0.9939	